

# Optimal capacity design of amine-based onboard CO<sub>2</sub> capture systems considering flexible ship operations

## **Authors:**

Juyoung Oh, Donghoi Kim, Simon Roussanaly, Rahul Anantharaman, youngsub Lim

*Date Submitted:* 2023-10-18

*Keywords:* Onboard carbon capture, MEA-based CO<sub>2</sub> capture process, Off-design performance, Ship engine load profile, Techno-economic assessment

## *Abstract:*

The International Maritime Organization has adopted a strategy aiming for net-zero greenhouse gas emissions from international shipping, prompting various mitigation technologies to comply with this strengthened strategy. Carbon capture technologies are increasingly being considered to satisfy the IMO strategy. In particular, amine-based carbon capture technologies, which are emerging as the most mature option, have been proposed for onboard application. However, the conventional design approach for onboard carbon capture systems, which assumes a fixed high engine load (75–100%), does not reflect flexible ship operation in a low engine load range, consequently leading to oversizing and unnecessary capital investment.

This study designs five MEA-based onboard carbon capture systems with different capacities (sizes) based on the exhaust gas conditions. The study investigates the off-design performance over the entire engine load range while maintaining the capacity of the capture systems at their design values. To identify the optimal capacity of the onboard carbon capture system, the off-design performance is applied to an actual sailing profile in order to quantify the energy requirement, potential CO<sub>2</sub> reduction rate, and capture cost.

The results show that smaller systems can reach a similar level of CO<sub>2</sub> reduction as other larger systems while reducing capture costs. This means that it is possible to reduce capture costs by decreasing the capture capacity while maintaining the carbon reduction potential. The small capacity capture system also achieves a more competitive CO<sub>2</sub> avoidance cost (235 € per tonne) compared to biofuel (304 € per tonne) for a similar CO<sub>2</sub> avoidance rate (59%). Thus, this study demonstrates a new approach to the design of amine-based onboard carbon capture systems considering flexible ship operations and presents the potential of the decarbonization technology for shipping industry.

*Record Type:* Preprint

*Submitted To:* LAPSE (Living Archive for Process Systems Engineering)

*Citation (overall record, always the latest version):*

LAPSE:2023.36829

*Citation (this specific file, latest version):*

LAPSE:2023.36829-1

*Citation (this specific file, this version):*

LAPSE:2023.36829-1v1

*License:* Creative Commons Attribution 4.0 International (CC BY 4.0)

# **Optimal capacity design of amine-based onboard CO<sub>2</sub> capture systems considering flexible ship operations**

Juyoung Oh<sup>a</sup>, Donghoi Kim<sup>b,\*</sup>, Simon Roussanaly<sup>b</sup>, Rahul Anantharaman<sup>b</sup>, Youngsub Lim<sup>a,\*\*</sup>

<sup>a</sup> Department of Naval Architecture and Ocean Engineering, Seoul National University, 1 Gwanak-ro, Gwanak-gu, Seoul, 08826, Republic of Korea

<sup>b</sup> SINTEF Energy Research, Trondheim, Norway

\* Corresponding author e-mail address: donghoi.kim@sintef.no (Donghoi Kim),

\*\* Corresponding author e-mail address: s98thesb@snu.ac.kr (Youngsub Lim)

## Abstract

The International Maritime Organization has adopted a strategy aiming for net-zero greenhouse gas emissions from international shipping, prompting various mitigation technologies to comply with this strengthened strategy. Carbon capture technologies are increasingly being considered to satisfy the IMO strategy. In particular, amine-based carbon capture technologies, which are emerging as the most mature option, have been proposed for onboard application. However, the conventional design approach for onboard carbon capture systems, which assumes a fixed high engine load (75–100%), does not reflect flexible ship operation in a low engine load range, consequently leading to oversizing and unnecessary capital investment. This study designs five MEA-based onboard carbon capture systems with different capacities (sizes) based on the exhaust gas conditions. The study investigates the off-design performance over the entire engine load range while maintaining the capacity of the capture systems at their design values. To identify the optimal capacity of the onboard carbon capture system, the off-design performance is applied to an actual sailing profile in order to quantify the energy requirement, potential CO<sub>2</sub> reduction rate, and capture cost. The results show that smaller systems can reach a similar level of CO<sub>2</sub> reduction as other larger systems while reducing capture costs. This means that it is possible to reduce capture costs by decreasing the capture capacity while maintaining the carbon reduction potential. The small capacity capture system also achieves a more competitive CO<sub>2</sub> avoidance cost (235 € per tonne) compared to biofuel (304 € per tonne) for a similar CO<sub>2</sub> avoidance rate (59%). Thus, this study demonstrates a new approach to the design of amine-based onboard carbon capture systems considering flexible ship operations and presents the potential of the decarbonization technology for shipping industry.

## Keywords

25 Onboard carbon capture; MEA-based CO<sub>2</sub> capture process; Off-design performance; Ship  
26 engine load profile; Techno-economic assessment

27 **Nomenclature**

28	CAPEX	Capital expenditures
29	CCS	Carbon capture and storage
30	CII	Carbon Intensity Indicator
31	DCC	Direct contact cooler
32	EEDI	Energy Efficiency Design Index
33	EEXI	Energy Efficiency Existing Ship Index
34	FAME	Fatty acid methyl ester
35	FOPEX	Fixed operating expenditures
36	GHG	Greenhouse gas
37	GTD	General Technical Data
38	IMO	International Maritime Organization
39	KPIs	Key performance indicators
40	LNG	Liquefied natural gas
41	L/G	Liquid-to-gas
42	MCR	Maximum continuous rating
43	MDEA	Methyldiethanolamine
44	MEA	Monoethanolamine

45	MEPC	Marine Environment Protection Committee
46	MGO	Marine gas oil
47	NG	Natural gas
48	NOAK	N <sup>th</sup> -of-a-kind
49	NRTL	Non-random two-liquid
50	OCC	Onboard carbon capture
51	OPEX	Operating expenditures
52	SFOC	Specific fuel oil consumption
53	SEC	Specific energy consumption
54	SRD	Specific reboiler duty
55	TCR	Total capital requirement
56	TDC	Total direct cost
57	TDCPC	Total direct cost including process contingency
58	TPC	Total plant cost
59	TEU	Twenty-foot equivalent unit
60	TRL	Technology readiness level
61	VOPEX	Variable operating expenditures
62	WHRU	Waste heat recovery unit
63		

## 64        **1. Introduction**

65        Global warming, which leads to drastic climate change, is largely influenced by CO<sub>2</sub>  
66        concentration and emissions. In 2022, the CO<sub>2</sub> concentration in the atmosphere reached its  
67        highest level in human history. According to data from the Scripps Institution of Oceanography,  
68        the CO<sub>2</sub> concentration measured at 421 ppm, which is 50% higher than the pre-industrial level  
69        [1]. Besides, global CO<sub>2</sub> emissions continued to increase from 34.8 billion tonnes in 2012 to  
70        36.6 billion tonnes in 2018. This upward trend can be partly attributed to the emissions from  
71        international shipping, which increased from 2.76% in 2012 to 2.89% of the global CO<sub>2</sub>  
72        emissions in 2018 [2]. Therefore, the International Maritime Organization (IMO) has  
73        established a first mandatory measure, the Energy Efficiency Design Index (EEDI), for  
74        greenhouse gas (GHG) reduction from international shipping [3]. Since its date of entry into  
75        force (1 January 2013), this legally binding regulation has been continuously tightened by  
76        advancing the start dates of implementation and further requiring its reduction targets [4]. In  
77        2018, the Marine Environment Protection Committee (MEPC) approved the Initial IMO  
78        Strategy to reduce GHG emissions from ships by at least 50% by 2050 compared to 2008 levels  
79        [5]. To achieve this strategy, the IMO has brought into effect new mandatory measures in 2022,  
80        including the Energy Efficiency Existing Ship Index (EEXI) as a technical measure and the  
81        Carbon Intensity Indicator (CII) as an operational measure [6,7]. Recently, the MEPC has  
82        adopted the 2023 IMO GHG Strategy, a strengthened revised strategy, which sets a target of  
83        net-zero GHG emissions by or around 2050 [8].

84        The shipping industry is making efforts to comply with the IMO strategy by switching to zero-  
85        carbon or carbon-neutral fuels [9]. However, the transition to these alternative fuels (e.g.,  
86        hydrogen, ammonia, methanol, biofuels) has limitations as an immediate solution because it  
87        requires a high technology readiness level (TRL) and comprehensive supporting infrastructure

88 [10]. Although conventional emission reduction strategies such as optimizing hull design and  
89 reducing ship speed have been implemented [9,11], these existing measures alone are  
90 insufficient to satisfy the IMO's ever-strengthening GHG strategy. Therefore, to meet the  
91 IMO's ambitious strategy, readily available reduction measures are required as interim  
92 technologies until alternative fuel solutions are established.

93 Carbon capture and storage (CCS) technologies have recently been considered to achieve the  
94 IMO strategy [12,13]. These proven technologies in land-based facilities [14] can be deployed  
95 on ships for onboard carbon capture and storage systems [15]. The onboard CCS systems  
96 capture CO<sub>2</sub> from the exhaust gas emitted from marine engines during the combustion of  
97 carbon-based fossil fuels (e.g., liquefied natural gas, marine diesel oil, heavy fuel oil), store the  
98 captured CO<sub>2</sub> onboard, and unload it at storage sites [16]. The four technologies considered for  
99 carbon capture applications are chemical absorption, adsorption, membrane separation, and  
100 cryogenic separation [17–20]. To decarbonize the shipping industry in a timely manner, many  
101 studies focus on solvent-based chemical absorption, which has the highest TRL compared to  
102 other candidates.

103 Luo and Wang [21] proposed a solvent-based onboard carbon capture system that uses  
104 monoethanolamine (MEA) solvent. Techno-economic assessments were performed for a cargo  
105 ship based on exhaust gas conditions emitted from four-stroke engines operating at 85% engine  
106 load. The results showed that a 73% carbon capture rate at a capture cost of 77.5 €/tonne CO<sub>2</sub>  
107 could be reached by using the existing system. The study also showed that installing an  
108 additional gas turbine could achieve a 90% carbon capture rate at a capture cost of 163 €/tonne  
109 CO<sub>2</sub>. Feenstra et al. [22] carried out techno-economic evaluations for onboard carbon capture  
110 systems for different engines (1280 kW and 3000 kW), solvents (monoethanolamine and  
111 piperazine), fuels (liquefied natural gas and diesel), carbon capture rates (60% and 90%), etc.

112 The analyses utilized exhaust gas data for four-stroke engines at 100% engine load. Lee et al.  
113 [23] investigated a chemical absorption process for onboard carbon capture using an activated  
114 methyldiethanolamine (aMDEA) solvent. They used exhaust gas conditions from a two-stroke  
115 low-pressure dual-fuel engine operating at 75% engine load. Long et al. [24] conducted process  
116 simulations and economic evaluations for ship-based carbon capture systems that were  
117 designed based on data from a four-stroke engine operating at 100% engine load. They showed  
118 improvements in the CO<sub>2</sub> capture rate, which was increased to 94.7%, by varying solvent  
119 selection and process configurations. Ji et al. [25] performed process simulations for MEA-  
120 based onboard carbon capture systems that assumed a liquefied natural gas (LNG) carrier  
121 consisting of four-stroke engines that operated at 85% engine load. They evaluated the carbon  
122 capture rate and energy consumption by varying the process parameters (solvents, packing type,  
123 liquid gas ratio, column design). Awoyomi et al. [26] analyzed process simulations and cost  
124 evaluations for an NH<sub>3</sub>-based onboard carbon capture system based on three different engine  
125 loads for 50%, 75%, and 85% of a four-stroke engine. The capital expenditures (CAPEX) for  
126 all different engine load cases were estimated only based on 85% engine load. The results  
127 indicated that a 90% carbon capture rate at a captured cost of 117 \$/tonne CO<sub>2</sub> was achieved.  
128 Ros et al. [27] conducted a techno-economic analysis of onboard carbon capture systems  
129 deployed on a semi-submersible crane vessel, the Sleipnir, powered by 12 four-stroke engines.  
130 They determined the equipment size of the onboard CCS systems based on the specific engine  
131 loads for the fictitious normalized operational ship profiles. The results presented a captured  
132 cost of 119 €/tonne CO<sub>2</sub> for a 72.5% carbon capture rate.

133 It should be noted that most of the onboard carbon capture (OCC) systems in previous studies  
134 have typically been designed based on the fixed engine load, assumed to be between 75% and  
135 100% of four-stroke engines, which are mainly used to power small ships (Table 1). However,  
136 the actual engine load varies continuously during the voyage due to various operating



137 conditions, such as route, speed, efficiency, market price, and weather. Besides, to reduce CO<sub>2</sub>  
138 emissions, the IMO recommends low average main engine loads for seaborne trade ships [28].  
139 This means that OCC systems are operated at off-design load conditions predominantly over  
140 the entire voyage, rather than constantly at a single high engine load. Thus, the conventional  
141 design approach to OCC systems can lead to over-dimensioning and unnecessary capital  
142 investment.

143 This study aims to design an OCC system that performs well over a wide range of engine  
144 loads while selecting a proper system capacity (size). In order to identify the optimal capacity  
145 of the OCC system, five amine-based OCC systems with different capacities are developed.  
146 The off-design performance of these systems is investigated under different engine load  
147 conditions, considering an actual load profile of the marine engine. These performance results  
148 are then quantified in terms of energy requirement, potential CO<sub>2</sub> reduction rate, and capture  
149 cost.

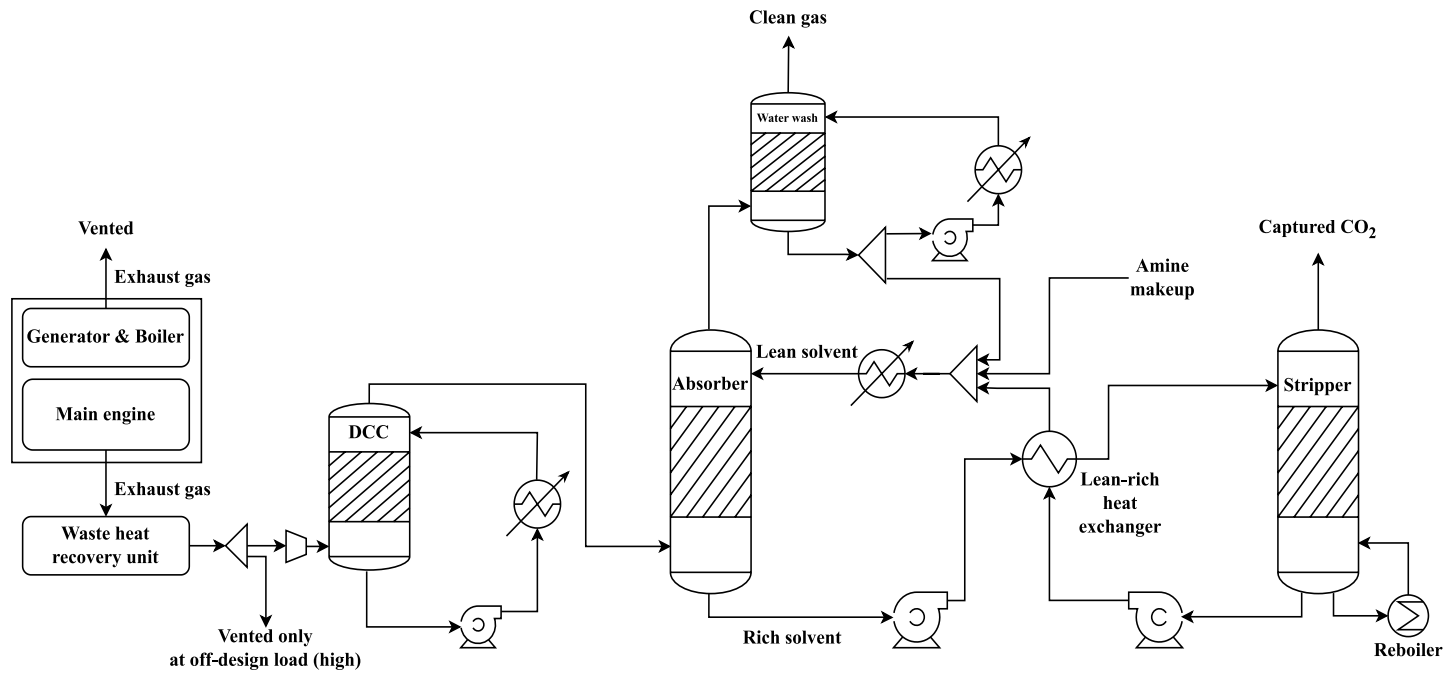
Table 1. Previous absorption-based onboard carbon capture studies.

Reference	Design-point load	Target engine	CO <sub>2</sub> concentration	Exhaust gas temperature (°C)
<b>Four-stroke engine</b>				
Luo and Wang [21]	85%	Wärtsilä 9L46 (Diesel)	5.69 mol%	362
Feenstra et al. [22]	100%	Wärtsilä 8L20DF (Diesel)	4.8 mol%	325
		Wärtsilä 8L20DF (LNG)	4.8 mol%	350
		Wärtsilä 6L34DF (Diesel)	4.8 mol%	381
		Wärtsilä 6L34DF (LNG)	4.8 mol%	381
Long et al. [24]	100%	Wärtsilä 6L34DF (Diesel)	4.8 mol%	381
Ji et al. [25]	85%	Wärtsilä 12V50DF (Diesel)	10.02 wt%	356
Awoyomi et al. [26]	85%	Wärtsilä 9L46DF (LNG)	7.6 wt%	362
Ros et al. [27]	60%, 71%	MAN 8L51/60DF (LNG)	4.47 vol%	405
<b>Two-stroke engine</b>				
Lee et al. [23]	75%	WinGD 6X72DF (LNG)	4.30 wt%	205
Stec et al. [29]	75%	MAN 6S50ME-C8.5 (HFO)	3.65 vol%	224
Einbu et al. [30]	66%	MAN 5S40ME-C9.5-GI (Diesel)	4.8 vol%	ca. 196
		MAN 5S40ME-C9.5-GI (LNG)	3.6 vol%	ca. 200

152        **2. Concept of this study**

153        In order to determine an OCC system with optimal capacity, this study designed amine-based  
154        OCC systems with five different capacities based on the exhaust gas conditions at the main  
155        engine loads of 50%, 60%, 70%, 80%, and 90%. To estimate the exhaust gas conditions, the  
156        ship's main engine was considered as the onboard emission source. Exhaust gases from  
157        auxiliaries such as generators and MGO-fired boilers were assumed to be vented without CO<sub>2</sub>  
158        capture. As the focus of this work was on designing the capture system considering flexible  
159        ship operation, the liquefaction and storage systems for the captured CO<sub>2</sub> were not included.  
160        Fig. 1 shows a process flow diagram of the amine-based OCC process that is the scope of this  
161        study.

162        Since the main engine load varies continuously during the voyage rather than constantly at a  
163        single high engine load, the OCC systems were analyzed in terms of both off-design  
164        performance and cumulative performance. The off-design performance at each off-design load  
165        was evaluated while maintaining the capacity of the capture systems at their design values. The  
166        main engine load profile was then used to quantify the cumulative performance for the entire  
167        voyage. Finally, the results were evaluated for each capacity scenario in terms of energy  
168        requirement, potential CO<sub>2</sub> reduction rate, and capture cost.



170

171

Fig. 1. Process flow diagram of the amine-based onboard carbon capture process.

172 **3. Case study**

173 **3.1 Targeted ship**

174 According to the results of the Third and the Fourth IMO GHG Studies, the CO<sub>2</sub> emissions  
175 from international shipping are dominated by three major ship types: containers, bulk carriers,  
176 and oil tankers. These ship types account for 51% and 55% of these emissions in 2012 and  
177 2018, respectively [2,31]. Thus, this study considered a container ship fueled by natural gas  
178 (NG) as the target ship to have a large impact on potential CO<sub>2</sub> reduction in the marine industry.  
179 The main specifications of the target ship are shown in Table 2 [32].

180

181 Table 2. Main specifications of the target ship [32].

Category	Unit	Value
Length over all	m	224.8
Breadth	m	37.5
Depth	m	19.1
Deadweight	DWT	53,200
Container capacity	TEU	3,840
Fuel	-	Natural gas
MCR <sub>Main engine</sub>	kW	18,200 (WinGD 6X72DF)

182

183 **3.2 Main engine exhaust gas conditions**

184 For OCC systems, it is challenging to attribute a single effect to one variable, given the  
185 complexity of the capture system including the interface with ship machineries. However, the

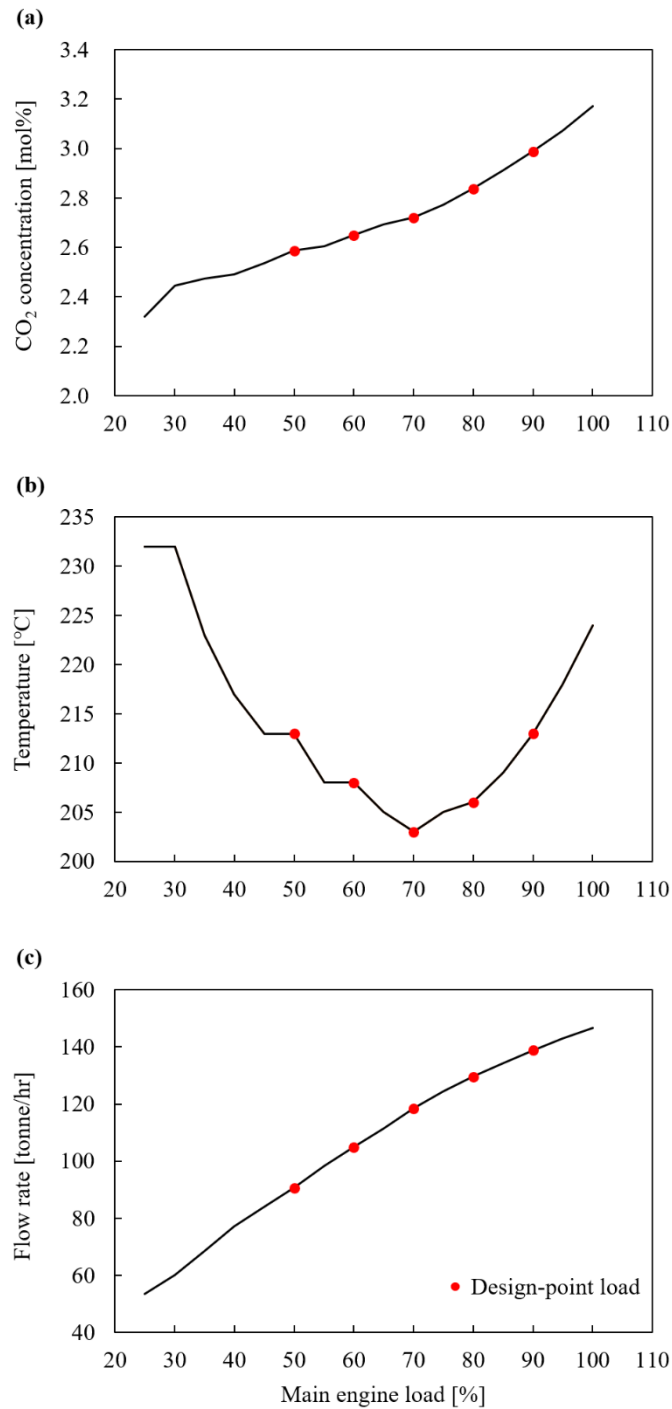
186 CO<sub>2</sub> concentration, temperature, and flow rate of the exhaust gas from a ship power system  
187 will have significant impacts on the sizing and energy consumption of onboard capture systems.

188 The CO<sub>2</sub> concentration of the exhaust gas from the main engine varies with fuel type, engine  
189 type (two-stroke or four-stroke), and engine load, typically ranging between approximately 3–  
190 6 mol% [21,23]. The main component of the energy required for CO<sub>2</sub> capture is the energy  
191 required to regenerate the solvent in the stripper and is referred to as specific reboiler duty –  
192 the energy required to capture 1 kg (or tonne) of CO<sub>2</sub>. The specific reboiler duty, which consists  
193 of the desorption heat ( $q_{\text{abs,co}_2}$ ), the heat required to increase the temperature of the solvent  
194 ( $q_{\text{sens}}$ ), and the heat required to generate the stripping steam ( $q_{\text{vap,H}_2\text{O}}$ ), is affected by the CO<sub>2</sub>  
195 concentration [33,34]. Thus, it is important to identify accurate CO<sub>2</sub> concentration in the  
196 exhaust gas with varying engine loads.

197 The exhaust gas temperature also varies depending on the fuel type, engine type, and engine  
198 load. The temperature determines the amount of heat that can be collected from the waste heat  
199 recovery unit (WHRU), which can be utilized for the capture system. Therefore, estimating  
200 exhaust gas temperature along with different engine loads is essential to evaluate the net energy  
201 required for the onboard capture system.

202 Given the size of container ships has been increasing [2], a two-stroke low-pressure dual-fuel  
203 engine (WinGD X-DF), mainly used to power large ships, was selected as the main engine for  
204 this study. The exhaust gas conditions were estimated using WinGD's General Technical Data  
205 (GTD) software for the 25–100% engine load range, the range provided by GTD. Fig. 2 shows  
206 that the two-stroke engine has a relatively low CO<sub>2</sub> concentration and exhaust gas temperature  
207 (avg. 2.7 mol%, 214 °C) compared to four-stroke engines (ca. 5 mol%, 325–405 °C). This  
208 means that additional fuel consumption is expected in the MGO-fired boiler to generate the  
209 extra heat to supply the reboiler, resulting in higher energy requirements and costs than those

210 reported in previous studies focusing on four-stroke engines. Thus, from a carbon capture  
211 perspective, these lower conditions may be the worst assumptions for the OCC case study.



212

213 Fig. 2. Exhaust gas conditions of the main engine: (a) CO<sub>2</sub> concentration of the exhaust gas as  
214 function of engine load; (b) Exhaust gas temperature as function of engine load; (c) Exhaust  
215 gas flow rate as function of engine load.

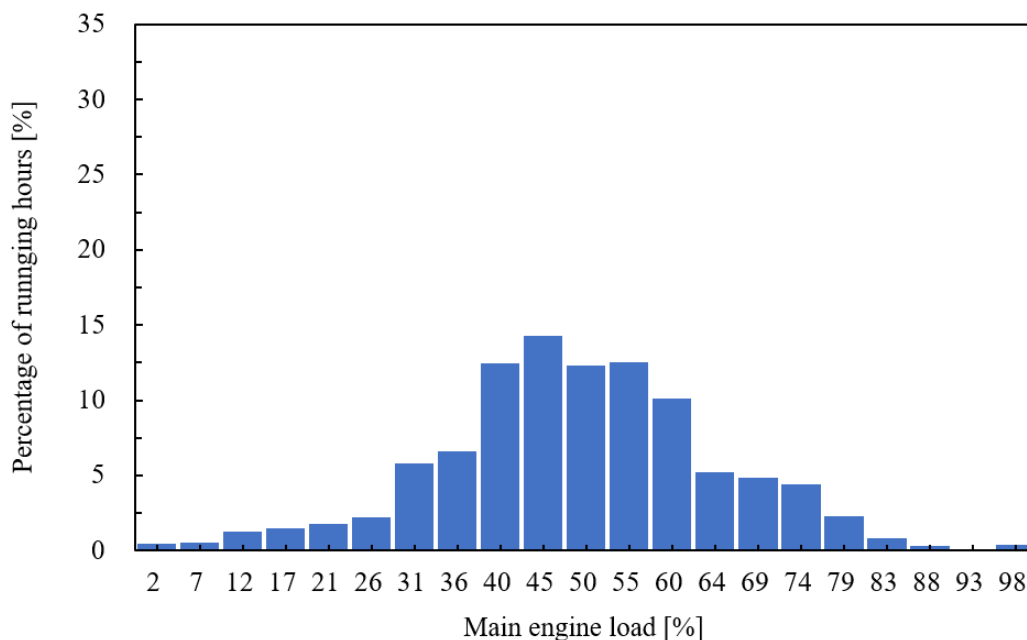
216

### 217 3.3 Main engine load profile

218 In 2018, most container fleets operated at lower engine loads than in 2012, with containers in  
219 the 3,000–4,999 TEU category operating at an average engine load of 33% [2]. This study  
220 adopted an actual main engine load profile with a low average engine load as in the IMO study.  
221 Fig. 3 shows a main engine load profile provided by a ship operator, Klaveness Combination  
222 Carriers. The target ship operates at an average engine load of 49%, not a high engine load.

223 Unlike land-based carbon capture systems in industrial facilities that typically operate at a  
224 relatively constant load, the main engine loads are not set at a specific point [27], but are varies  
225 between 36% and 60% load, as shown in Fig. 3. It should be noted that the marine engine is  
226 operated in the low engine load range for most of the voyage.

227



228

229 Fig. 3. Main engine load distribution of eight CLEANBU combination carriers from  
230 Klaveness Combination Carriers.



231 **4. Onboard carbon capture system**

232 **4.1 Capacity scenarios**

233 The existing design methodology for OCC systems has focused on a fixed high engine load  
 234 (75–100%). However, this approach has overlooked typical ship operations that frequently  
 235 operate in low engine load ranges. In order to reflect the actual main engine load profile, five  
 236 capacity scenarios were defined based on the exhaust gas conditions at engine loads of 50%,  
 237 60%, 70%, 80%, and 90%, as shown in Table 3. Thus, in this work, five different amine-based  
 238 OCC systems were designed according to their capacity scenarios. For example, in capacity  
 239 scenario 1, the OCC system is designed based on the exhaust gas generated from the main  
 240 engine at 50% load, which is the design-point load of capacity scenario 1.

241

242 Table 3. Capacity scenarios for the design and operation of onboard carbon capture systems.

Category	Unit	Capacity scenario 1	Capacity scenario 2	Capacity scenario 3	Capacity scenario 4	Capacity scenario 5
Design-point load	%	50	60	70	80	90
Feed flow rate	tonne/hr	90.59	104.88	118.45	129.51	138.77
CO <sub>2</sub>	mol%	2.59	2.65	2.72	2.84	2.99
H <sub>2</sub> O		5.15	5.28	5.42	5.66	5.96
N <sub>2</sub>		77.04	76.99	76.93	76.84	76.72
O <sub>2</sub>		15.22	15.08	14.92	14.66	14.33
Exhaust gas temperature	°C	213	208	203	206	213
Off-design load						
High	-	Engine loads higher than the design-point load				
Low	-	Engine loads lower than the design-point load				

243

## 244           **4.2 Process design at design-point loads**

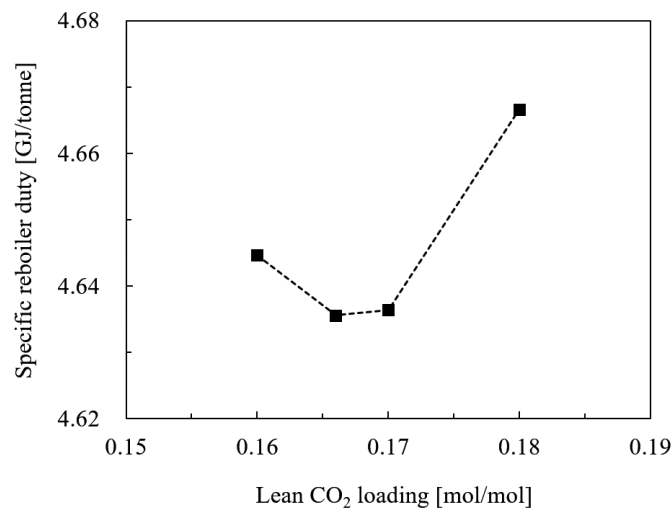
245       In this study, an aqueous solution of 30 wt% monoethanolamine (MEA) was selected as a  
246 solvent. Aqueous MEA solution is the most studied amine solvent for CO<sub>2</sub> capture [34]. The  
247 rigorous process models of the MEA-based capture process for design-point loads were  
248 developed based on the rate-based separation column model in Aspen Plus version 11 [35],  
249 which uses the unsymmetric electrolyte non-random two-liquid (NRTL) activity coefficient  
250 model for liquid properties and PC-SAFT equation of state for vapor properties. To improve  
251 the reliability of the rate-based models operating under onboard conditions, the carbon capture  
252 process model was validated against the pilot plant data reported by Notz et al. [34]. The  
253 validation results are presented in Appendix A.

254       Based on the validated model, the scale-up model of OCC systems was developed. These  
255 systems consist of three main columns: a direct contact cooler (DCC), an absorber including a  
256 water washing section, and a stripper, as shown in Fig. 1. The DCC, installed upstream of the  
257 absorber, cools the exhaust gas that has passed through a WHRU because the CO<sub>2</sub> absorption  
258 in an aqueous MEA solution is more favorable at lower exhaust gas temperatures. It can also  
259 reduce the volume flow rate of the exhaust gas, which affects the size of the columns. The  
260 exhaust gas, cooled to about 45 °C via the DCC, enters the absorber and the CO<sub>2</sub> in the exhaust  
261 gas is absorbed into the lean (regenerated) amine solvent. The scrubbed gas from the top of the  
262 absorber is washed through the water washing section to minimize amine losses before being  
263 vented as clean gas. The rich amine solvent, which leaves the bottom of the absorber, passes  
264 through a lean-rich heat exchanger and enters the stripper. Then, the CO<sub>2</sub> in the rich amine  
265 solvent is desorbed by the heat input through a reboiler in the stripper. Finally, the captured  
266 CO<sub>2</sub> is obtained from the top of the stripper while the hot regenerated solvent from the bottom  
267 of the stripper passes through the lean-rich heat exchanger and circulates back to the absorber.

268 Considering the exhaust gas conditions of each design-point load (Table 3), the sizes of three  
269 main columns were determined for each capacity scenario. However, the packing height of the  
270 columns was fixed considering the limited space on the ship and the operation of marine radar.  
271 The diameter of the columns was determined based on the flooding parameter of 70% [36],  
272 which is influenced by the lean CO<sub>2</sub> loading.

273 The lean CO<sub>2</sub> loading with the lowest energy consumption was investigated for each design-  
274 point load condition while maintaining the base carbon capture rate of 90% [37,38] as shown  
275 in Fig. 4. The flow rate of the lean amine solvent was estimated based on the energy-optimal  
276 lean CO<sub>2</sub> loading value for the solvent. Therefore, in the process design at design-point loads,  
277 column diameters and lean CO<sub>2</sub> loading were defined according to the design-point conditions  
278 of each capacity scenario. The design data of different capacity scenarios, used for both design-  
279 point and off-design operations, were determined, as shown in Table 4.

280



281

282 Fig. 4. Variation of specific reboiler duty with lean CO<sub>2</sub> loading for the design-point  
283 conditions of capacity scenario 1.

284

285

Table 4. Design data for each capacity scenario.

Category	Unit	Capacity	Capacity	Capacity	Capacity	Capacity
		scenario 1	scenario 2	scenario 3	scenario 4	scenario 5
Lean CO <sub>2</sub> loading	mol/mol	0.166	0.166	0.166	0.168	0.168
Base CO <sub>2</sub> capture rate	%			90		
DCC packing height	m			5		
Absorber, stripper packing height	m			10		
Water washing section packing height	m			1		
DCC diameter	m	3.72	4.01	4.28	4.50	4.69
Absorber diameter	m	3.21	3.46	3.68	3.87	4.03
Stripper diameter	m	1.22	1.32	1.42	1.50	1.58
Water washing section diameter	m	3.62	3.89	4.15	4.34	4.49
MEA concentration	wt%			30		
Exhaust gas temperature after WHRU	°C			140		
Lean solvent temperature to absorber	°C			40		
Lean-rich heat exchanger minimum temperature approach	°C			10		
Cooling water temperature	°C			30		
Absorber operating pressure	atm			1		
Stripper operating pressure	atm			2		
Captured CO <sub>2</sub> purity	mol%			95		

286

287

### 4.3 Off-design operations

288

289

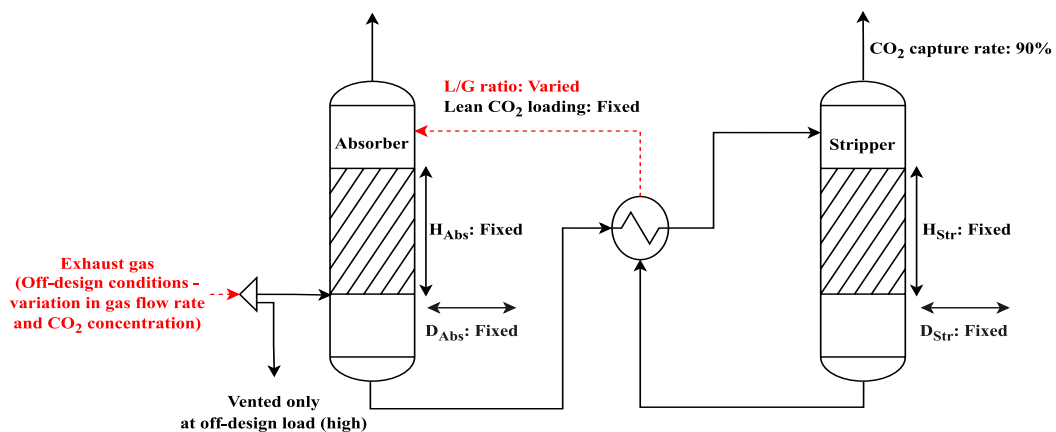
290

In this study, the OCC systems were operated and analyzed under varying engine loads (Fig. 3). The off-design operations were performed by varying only the flow rate of the lean amine solvent to capture 90% of the CO<sub>2</sub> emitted from different main engine loads (with varying gas

291 flow rate and CO<sub>2</sub> concentration) while maintaining the design data from the corresponding  
292 capacity scenario (Table 4).

293 However, there is a limit to the operating range of the given absorber design from each  
294 capacity scenario due to fluid dynamic reasons [34]. The upper limit of the exhaust gas flow  
295 rate was determined to be the flow rate emitted at each design-point load. At higher engine  
296 loads than the design-point load, i.e., off-design loads (high), only the exhaust gas flow rate  
297 corresponding to the specified design-point load was fed to the absorber. The excess flow was  
298 vented from the original exhaust gas before entering the absorber, as shown in Fig. 5.

299



300

301

Fig. 5. Off-design operation.

302

303 The lower limit of the exhaust gas flow rate that a column can handle was decided by the  
304 turndown ratio of a liquid distributor in a packed column, which is defined as the ratio of the  
305 maximum lean solvent flow rate to the minimum lean solvent flow rate. Thus, the exhaust gas  
306 flow rate that can be handled with the minimum lean solvent flow rate was defined as the lower  
307 limit of the exhaust gas flow rate. The typical turndown ratio ranges from 2:1 to 3:1 [39–41],

308 which can be increased by using a dual liquid distributor [40]. However, for ship applications,  
309 it is not suitable to implement the multiple-stage distributor due to height limitations. Therefore,  
310 a turndown ratio of 2.5:1 was used in this study considering the limited height on the ship,  
311 motion dynamics, and fluid dynamic parameters [39].

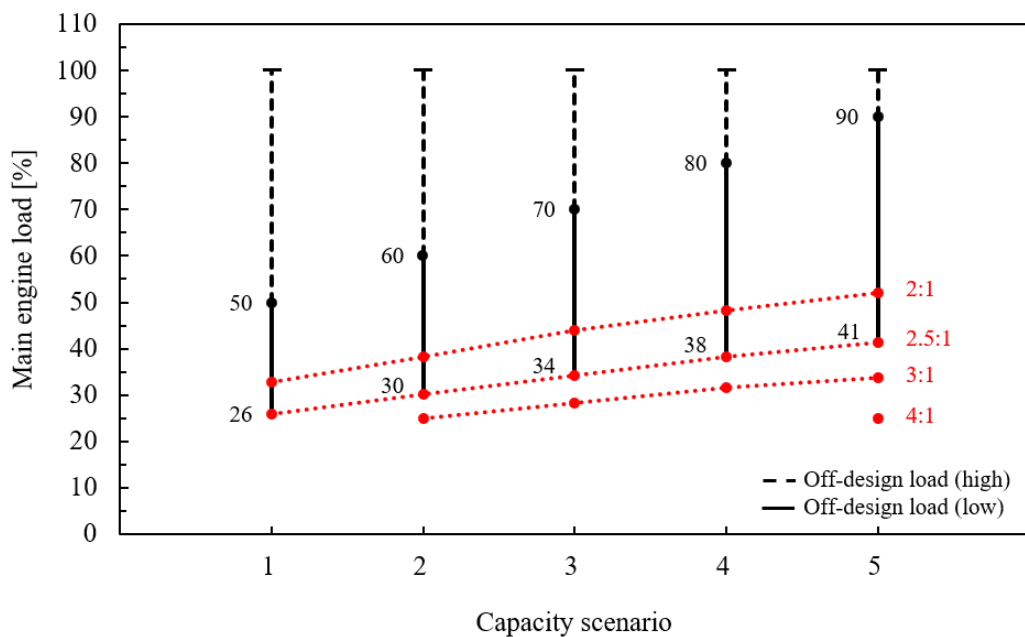
312 The maximum lean solvent flow rate was observed at 100% engine load for all capacity  
313 scenarios. At 100% engine load, the exhaust gas flow rate entering the column was the same  
314 as the flow rate at each design-point load. However, the CO<sub>2</sub> concentration at off-design loads  
315 (high) was higher than the design-point values, requiring a larger lean solvent flow rate. After  
316 identifying the maximum lean solvent flow rate for each capacity scenario, the minimum lean  
317 solvent flow rate that could be distributed by the liquid distributor was calculated considering  
318 the turndown ratio. This minimum lean solvent flow rate was used to determine the lower limit  
319 of the exhaust gas flow rate (main engine load) entering the capture system.

320 Since the carbon capture process models were simulated assuming that all process models  
321 could be operated over the 25–100% engine load range, the available operating range  
322 depending on turndown ratios could also be estimated. The OCC system designed for capacity  
323 scenario 5 required a 4:1 turndown ratio to handle the 25–100% engine load range, while the  
324 system designed for capacity scenario 1 could cover the similar engine load range with a much  
325 lower turndown ratio (2.5:1). Thus, at low turndown ratios, larger capacity systems may have  
326 limitations in covering a low engine load range due to a narrower operating range compared to  
327 their smaller counterparts.

328 The corresponding engine loads of the operating ranges and minimum engine loads for  
329 different turndown ratios are illustrated in Fig. 6. With the 2.5:1 turndown ratio, the capacity  
330 scenario 1 can be operated for the engine load ranges of 26–100% while capacity scenario 5  
331 can covers 41–100% engine load. It is worth noting that when the engine load is over the design

332 point, such as 51–100% load for the capacity scenario 1 and 91–100% load for capacity  
333 scenario 5, the excess flow was vented. In addition, the exhaust gas emitted below the minimum  
334 engine load, which the column could not handle, was also vented.

335



336

337 Fig. 6. Main engine load range in which the onboard carbon capture system can be operated  
338 for each capacity scenario (black circles represent the design-point load and red circles  
339 indicate minimum engine loads depending on the different turndown ratios).

340

341

342

343

344 **5. Key performance indicators**

345 This section describes the key performance indicators (KPIs) used to evaluate the  
346 performance of OCC systems. The main engine load profile was used to integrate the off-design  
347 performance from the design-point and off-design operations for each capacity scenario to  
348 quantify the KPIs: CO<sub>2</sub> reduction, energy requirements, and costs for the entire voyage.

349 **5.1 CO<sub>2</sub> reduction**

350 The average CO<sub>2</sub> generated over a single voyage, including the CO<sub>2</sub> from the carbon capture  
351 systems, is calculated as:

352

$$\begin{aligned} \text{CO}_2 \text{ generated (total) [tonne/hr]} & \\ & = \text{CO}_2 \text{ generated (main engine)} + \text{CO}_2 \text{ generated (additional)} \end{aligned} \quad (1)$$

353

354 where this equation is divided into two emission sources: the CO<sub>2</sub> generated (main engine) by  
355 the main engine (WinGD 6X72DF) and the CO<sub>2</sub> generated (additional) by the generator and  
356 the MGO-fired boiler. These auxiliary units are responsible for producing electricity and  
357 additional heat for the carbon capture systems. For the term CO<sub>2</sub> generated (main engine), to  
358 obtain the CO<sub>2</sub> emissions for the entire voyage (0–100%), the CO<sub>2</sub> emissions below 25%  
359 engine load were extrapolated based on the CO<sub>2</sub> emission data from the 25% to 100% engine  
360 load range. Thus, the CO<sub>2</sub> generated (main engine) was evaluated for the entire voyage, while  
361 the second term, CO<sub>2</sub> generated (additional), was estimated only when in operation. To  
362 calculate the CO<sub>2</sub> generated (additional), the additional energy used by the generator and MGO-  
363 fired boiler was converted to equivalent marine gas oil (MGO) consumption. This additional  
364 fuel consumption was then multiplied by the emission factor, as shown below:



365

CO<sub>2</sub> generated (additional)

$$\begin{aligned} &= (\text{Additional energy (generator) [GJ}_e] \times \text{SFOC} \\ &+ \frac{\text{Additional energy (MGO – fired boiler) [GJ}_{th}]}{\text{Boiler efficiency} \times \text{LHV}_{\text{MGO}}}) \times \text{EF}_f \end{aligned} \quad (2)$$

366

367 where the specific fuel oil consumption (SFOC) of the generator was obtained from the diesel  
368 engine (WinGD 5X35-B). The assumptions used to calculate the emissions are shown in Table  
369 5.

370

371 Table 5. Assumptions used for estimating additional carbon emissions.

Category	Unit	Value
SFOC of generator	tonne/GJ	0.047
Boiler efficiency	%	85
LHV <sub>MGO</sub>	GJ/tonne	42.7 [42]
Emission factor (EF <sub>f</sub> )	tonne <sub>CO<sub>2</sub></sub> /tonne <sub>Fuel</sub>	3.206 [2]

372

373 The average CO<sub>2</sub> emitted after operation of the carbon capture systems is calculated as:

374

$$\text{CO}_2 \text{ emitted [tonne/hr]} = \text{CO}_2 \text{ generated (total)} - \text{CO}_2 \text{ captured} \quad (3)$$

375

376 where the CO<sub>2</sub> captured is also obtained within the available operating range of the column.

377 The CO<sub>2</sub> avoided quantifies the actual CO<sub>2</sub> removal performance by introducing the capture  
378 systems. Therefore, this cumulative performance provides the CO<sub>2</sub> reduction for a single  
379 voyage with the OCC systems, as shown below:

380

$$\text{CO}_2 \text{ avoided [tonne/hr]} = \text{CO}_2 \text{ generated (main engine)} - \text{CO}_2 \text{ emitted} \quad (4)$$

381

$$\text{CO}_2 \text{ avoided rate [\%]} = \frac{\text{Cumulative CO}_2 \text{ avoided}}{\text{Cumulative CO}_2 \text{ generated (main engine)}} \times 100 \quad (5)$$

382

383 where the CO<sub>2</sub> generated (main engine) and CO<sub>2</sub> emitted are the CO<sub>2</sub> emissions of the target  
384 ship without and with the carbon capture systems, respectively.

385

## 386 **5.2 Energy requirements**

387 As mentioned earlier, the specific reboiler duty (SRD) was defined as the reboiler energy  
388 required to capture 1 tonne of CO<sub>2</sub>. However, in order to reach the base carbon capture rate of  
389 90%, additional energy was generated in the MGO-fired boiler to supply the reboiler. Thus, the  
390 specific energy consumption (SEC) is defined as the specific additional energy for the reboiler.  
391 The cumulative SEC of CO<sub>2</sub> avoided quantifies net energy requirements for a single voyage  
392 with the OCC systems. It is measured by cumulative indicators of additional energy and CO<sub>2</sub>  
393 avoided, as shown below:

394

$$\begin{aligned} & \text{Cumulative SEC of CO}_2 \text{ avoided [GJ}_{\text{th}}\text{/tonne CO}_2 \text{ avoided]} \\ & = \frac{\text{Cumulative reboiler heat duty required} - \text{Cumulative waste heat recovery}}{\text{Cumulative CO}_2 \text{ avoided}} \quad (6) \end{aligned}$$

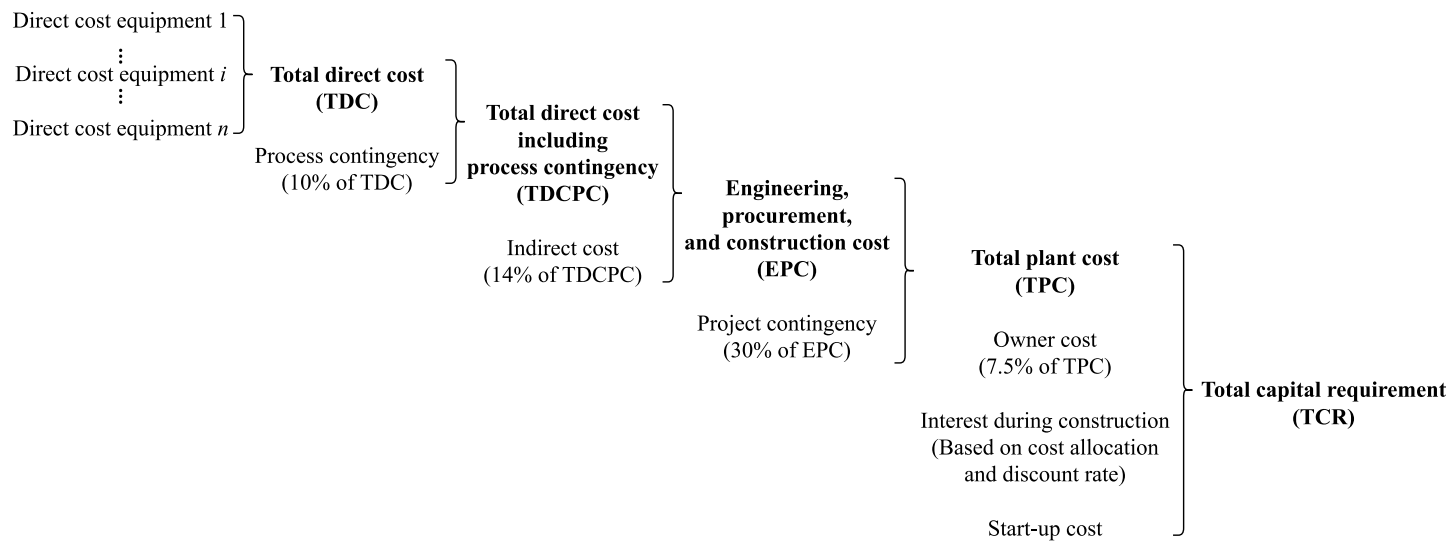
395

396 where the waste heat recovery is calculated cumulatively within the available operating range  
397 of the column.

398

### 399 **5.3 Cost evaluation**

400 The MEA-based OCC systems were evaluated on an N<sup>th</sup>-of-a-kind (NOAK) basis, i.e.,  
401 assuming a point in time when the technology is commercially mature [43]. The CAPEX was  
402 estimated using a bottom-up costing methodology, as shown in Fig. 7 [44,45]. Aspen Process  
403 Economic Analyzer<sup>®</sup> was used to calculate the direct costs of process equipment (e.g., packed  
404 columns, pumps, heat exchangers, blower). The total direct cost including process contingency  
405 (TDCPC) was determined using a process contingency factor, which was set to 10% of the total  
406 direct cost (TDC). Then, the engineering, procurement, and construction cost (EPC) was  
407 calculated by summing up the TDCPC and indirect costs (set to 14% of TDCPC). The total  
408 plant cost (TPC) was calculated by summing up the EPC and project contingencies (set to 30%  
409 of EPC). Finally, the total capital requirement (TCR) was obtained by adding the owner costs  
410 (set to 7.5% of TPC), interest during construction, start-up costs, and the TPC.



411

412

413

Fig. 7. Bottom-up costing methodology for CAPEX estimation [44].

414 The OPEX is the sum of fixed OPEX (FOPEX) and variable OPEX (VOPEX). The annual  
 415 FOPEX includes maintenance (set to 2.0% of TPC), insurance and local taxes (set to 2.0% of  
 416 TPC), and labor costs. The labor cost was estimated based on the assumption of an annual  
 417 salary of 60,000 € per operator and employing a total of 5 operators. The annual VOPEX is  
 418 estimated taking into account the utility costs, including fuel, process water, and solvent make-  
 419 up. Currently, fuel prices have risen globally due to the COVID-19 pandemic in late 2019 and  
 420 the Russia-Ukraine war in February 2022. The current MGO price has significantly increased  
 421 to 712 € per tonne compared to the yearly averages of 508 and 482 € per tonne observed in  
 422 2019 (pre-COVID) and 2021 (Russia-Ukraine war), respectively. In order to observe the CO<sub>2</sub>  
 423 avoidance costs as fuel prices vary, VOPEX was calculated based on fuel prices in 2019 (pre-  
 424 COVID) and 2021 (pre-war), respectively. The utility costs are shown in Table 6.

425

426

Table 6. Costs of utilities for VOPEX [46–48].

Category	Year	Unit	Value
MGO	2019	€/tonne	508
	2021	€/tonne	482
	2023	€/tonne	712
LNG	2019	€/tonne	400 [27]
	2021	€/tonne	858
	2023	€/tonne	855
FAME	2019	€/tonne	779
	2021	€/tonne	1405
	2023	€/tonne	1270
Process water	-	€/m <sup>3</sup>	6.65
MEA	-	€/tonne	1600

427

428 The CO<sub>2</sub> avoidance cost is the KPI used to evaluate the cost performance of MEA-based OCC  
 429 systems. The CO<sub>2</sub> avoidance cost is calculated as [45,49]:

430

CO<sub>2</sub> avoidance cost [€/tonne CO<sub>2</sub> avoided]

$$= \frac{\text{Annualized CAPEX} + \text{Annual FOPEX} + \text{Annual VOPEX}}{\text{Annual CO}_2 \text{ avoided}} \quad (7)$$

431

432 The annual CO<sub>2</sub> avoided was estimated based on the operating hours per year and the average  
 433 CO<sub>2</sub> avoided over a single voyage. The assumptions used to calculate the CO<sub>2</sub> capture cost are  
 434 shown in Table 7.

435

436 Table 7. Assumptions used for calculating carbon capture cost.

Category	Unit	Value
Economic lifetime (ship)	year	25
Annual number of round trips	-	10
Average time per round trip	hr	744.6
Operating hours	hr/year	7446
Discount rate	%	8

437

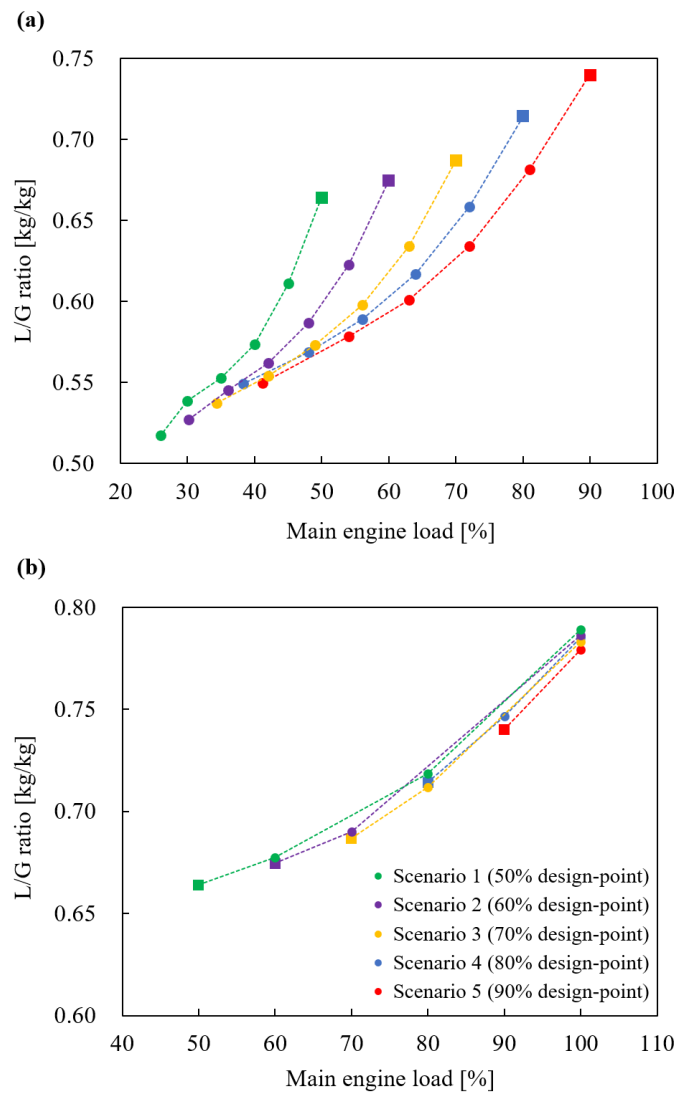
438

439        **6. Results and discussion**

440        **6.1 Off-design performance of case study**

441        As shown in Fig. 8 and Fig. 9, the liquid-to-gas (L/G) ratios and SRD were plotted over the  
442        available operating range for each capacity scenario. In Fig. 8, the L/G ratio increases as the  
443        design-point load increases. The high CO<sub>2</sub> concentration at the absorber feed stream and the  
444        high carbon capture rate contribute to a high L/G ratio [37,50]. As previously mentioned, the  
445        L/G ratios were determined to achieve the base carbon capture rate of 90% for all operations.  
446        With the base capture rate constant, an increase in engine load increased the CO<sub>2</sub> concentration  
447        (Fig. 2), which subsequently resulted in a higher L/G ratio (higher lean solvent flow rate). For  
448        the same reason, the L/G ratios of the off-design loads (low) for each capacity scenario are  
449        lower than the L/G ratios of their design-point loads, as shown in Fig. 8(a). Also, the L/G ratios  
450        of the off-design load (high) ranges follow the same trend as the CO<sub>2</sub> concentration increases,  
451        as shown in Fig. 8(b).

452



453

454 Fig. 8. Variations of L/G ratio with main engine load for different capacity scenarios: (a) L/G  
 455 ratios for design-point load ranges and off-design load (low) ranges; (b) L/G ratios for off-  
 456 design load (high) ranges (Squares are for design-point loads and circles are for off-design  
 457 loads).

458

459 Fig. 9 shows that the SRD, which does not consider the waste heat recovery and the CO<sub>2</sub>  
 460 generated (additional), gradually decreases as the design-point load increases. This trend,  
 461 which is opposite to the L/G ratio results, can also be explained by the CO<sub>2</sub> concentration  
 462 [33,34,50,51]. As discussed earlier, the specific reboiler duty comprises three components:

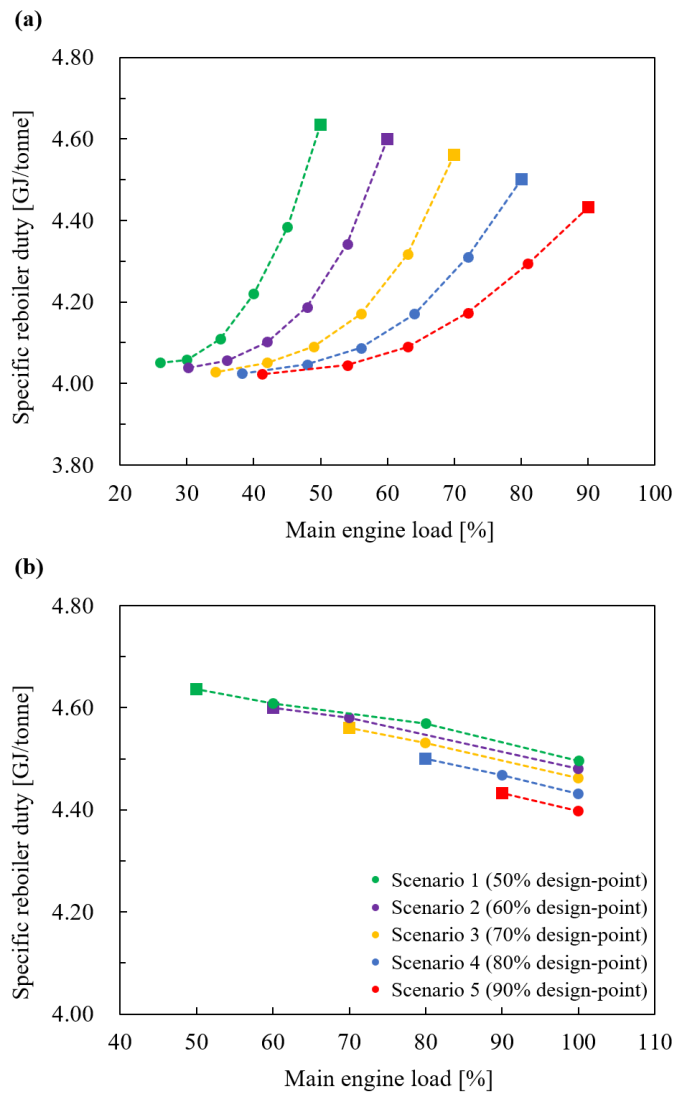


463  $q_{\text{abs,CO}_2}$ ,  $q_{\text{sens}}$ , and  $q_{\text{vap,H}_2\text{O}}$ . The contributions of these three components to the specific  
464 reboiler duty were estimated, as shown in Fig. 10. Comparing the energy requirements between  
465 capacity scenario 1 and capacity scenario 5, the most significant reduction is observed in the  
466 heat required to generate the stripping steam ( $q_{\text{vap,H}_2\text{O}}$ ). This is because increasing the CO<sub>2</sub>  
467 concentration at the absorber feed stream increased both the lean and rich CO<sub>2</sub> loadings, as  
468 shown in Table 4 and Fig. 11, respectively. Correspondingly, the water concentration at the  
469 stripper feed stream decreased. Therefore, a relatively smaller amount of stripping steam was  
470 required compared to the lower design-point load. For the same reason, the SRD at the off-  
471 design loads (high) follows the same trend with increasing engine load (increasing CO<sub>2</sub>  
472 concentration), as shown in Fig. 9(b).

473 However, it is worth noting that the SRD decreases at lower loads (off-design load conditions)  
474 even though the CO<sub>2</sub> concentration in the exhaust gas is reduced. At the off-design loads (low),  
475 a lower flow rate of the exhaust gas enters the capture system while the column dimensions are  
476 maintained from the design values. As indicated in Fig. 12, the reduced feed flow rate leads to  
477 a relatively larger interfacial area and a higher rich CO<sub>2</sub> loading, resulting in a lower SRD. This  
478 trend is also observed in the pilot plant data reported by Notz et al. [34].

479 The off-design performance indicates that larger capacity capture systems benefit from a  
480 lower SRD. Therefore, a cumulative analysis is required to identify the actual capture potential  
481 and energy requirements of OCC systems over an entire voyage.

482



483

484

Fig. 9. Variations of specific reboiler duty with main engine load for different capacity

485

scenarios: (a) SRD for design-point load ranges and off-design load (low) ranges; (b) SRD

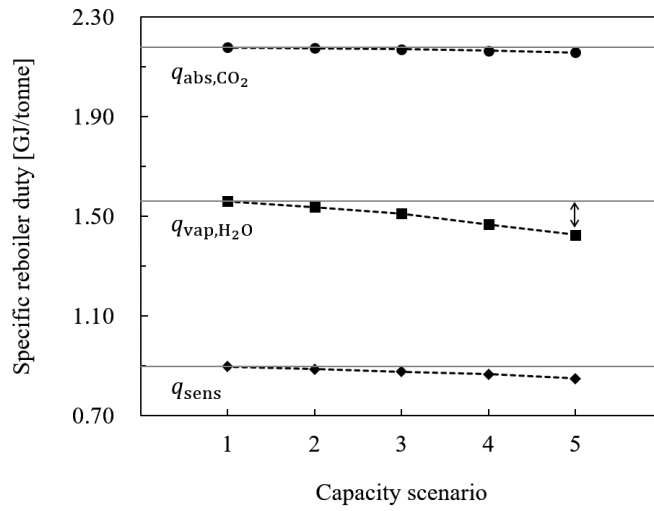
486

for off-design load (high) ranges (Squares are for design-point loads and circles are for off-

487

design loads).

488



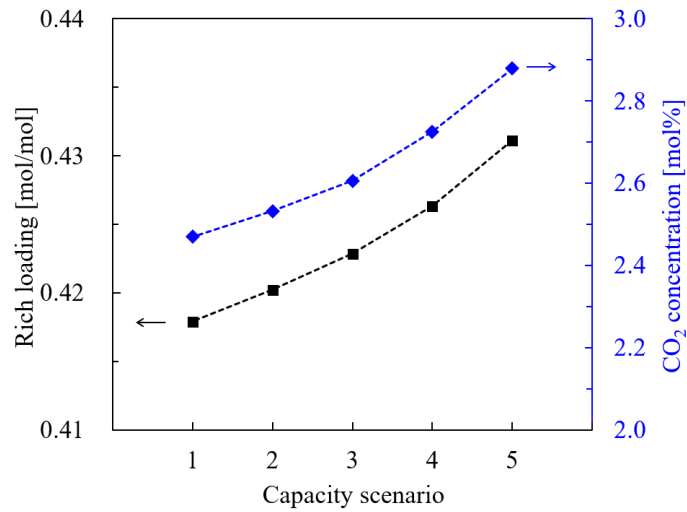
489

490 Fig. 10. Contributions to specific reboiler duty at design-point load for each capacity

491

scenario.

492



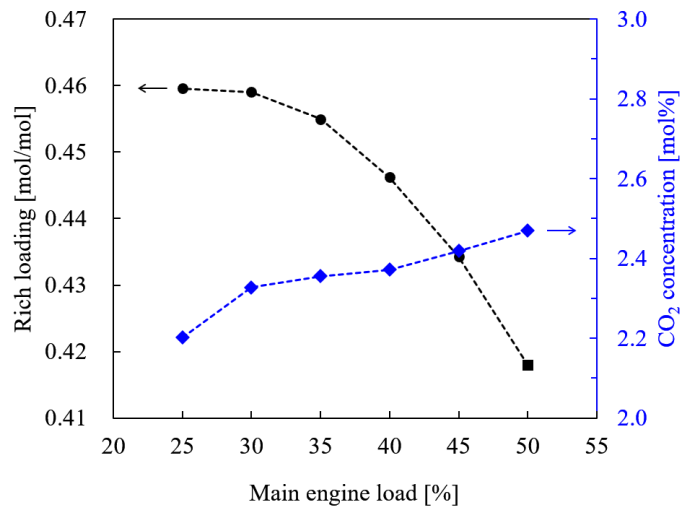
493

494 Fig. 11. Variations of rich loading with CO<sub>2</sub> concentration at design-point load for each

495

capacity scenario.

496



497

498 Fig. 12. Variations of rich loading and CO<sub>2</sub> concentration with main engine load for capacity  
 499 scenario 1.

500

## 501 6.2 Cumulative performance of case study

502 Using the actual main engine load profile and the off-design performance, the cumulative  
 503 performance for each capacity scenario for the entire voyage were quantified in terms of the  
 504 following KPIs: CO<sub>2</sub> avoided rate, cumulative SEC, and CO<sub>2</sub> avoidance cost. As can be seen  
 505 in Table 8, the OCC systems designed based on capacity scenarios 1–5 indicate a similar level  
 506 of carbon reduction potential with a marginal deviation. Even smaller OCC systems achieve  
 507 comparable emission reductions due to the low average main engine load of the target ship and  
 508 the wide operating range of the absorber. However, larger OCC systems have a lower  
 509 cumulative SEC than the systems based on capacity scenarios 1 and 2 due to their relatively  
 510 larger interfacial area as explained in the previous section. The same trend is observed in the  
 511 VOPEX, which is proportional to the energy consumption of the capture system.

512 However, it should be noted that the systems based on low-capacity scenarios benefit from a  
 513 lower CAPEX as the capacity of the capture system decreases. Besides, the cumulative analysis

514 shows that the CAPEX savings from a reduced capacity of the capture system outweigh the  
515 OPEX penalties, resulting in a lower CO<sub>2</sub> avoidance cost. For example, the system based on  
516 capacity scenario 1 has a 22% decrease in CAPEX while VOPEX increases only by 6%  
517 compared to the system based on capacity scenario 5, resulting in the lowest CO<sub>2</sub> avoidance  
518 cost (232 € per tonne). For the system based on capacity scenario 2, which has the highest CO<sub>2</sub>  
519 avoided rate, its compact size results in a 19% reduction in CAPEX compared to the system  
520 based on capacity scenario 5, leading to an 8% decrease in CO<sub>2</sub> avoidance cost (235 € per  
521 tonne).

522 The CO<sub>2</sub> avoidance costs estimated from this work with the two-stroke engine are found to  
523 be higher than those reported in previous studies based on four-stroke engines. The two-stroke  
524 engine has a lower CO<sub>2</sub> concentration and less recoverable waste heat than four-stroke engines.  
525 This results in higher fuel consumption for additional energy generation, which directly  
526 increases the OPEX of the capture system. Consequently, for OCC systems with two-stroke  
527 engines, both CAPEX and OPEX emerge as significant contributors to the total capture cost  
528 while previous studies with four-stroke engines indicate the CAPEX to be the main driver of  
529 the economic performance [22,26,27]. The importance of OPEX can also be seen in the report  
530 by OGCI and Stena Bulk [52]. They conducted a case study on a two-stroke engine with low  
531 waste heat availability that shows a similar level of avoidance costs to this study.

532 Thus, as one of key parameters affecting the capture cost, the fuel price (VOPEX) needs to be  
533 considered when investigating the viability of an OCC system with two-stroke engines. In  
534 particular, three different fuel prices are assumed in this work, reflecting the recent volatility  
535 of MGO prices. As can be seen in Fig. 13, the OPEX is significantly affected by fuel prices.  
536 Given that the OPEX is the major component of the total capture cost, fuel prices also become  
537 a crucial parameter. Currently, high fuel prices have resulted in increased capture costs, but if

538 fuel prices were to return to pre-COVID levels, the CO<sub>2</sub> avoidance cost for the systems based  
539 on low-capacity scenarios could drop to around 200 € per tonne.

540 In addition, to compare the amine-based carbon capture system with an alternative measure,  
541 CO<sub>2</sub> avoidance costs for the use of FAME (fatty acid methyl ester) were also calculated. FAME  
542 is the most widely used biofuel in the marine sector [53] and can be operated in existing engines  
543 without major modification. In this estimation, FAME was used until it achieved the CO<sub>2</sub>  
544 avoided rate of 59%, which is the highest CO<sub>2</sub> avoided rate of the OCC systems in this work,  
545 and only considers the operating cost according to the FAME consumption. However, the  
546 alternative technology using FAME is not competitive with amine-based systems, as shown in  
547 Fig. 13. Based on the average annual price in 2023, it was calculated at 304 € per tonne, which  
548 is 30% higher than the CO<sub>2</sub> avoidance cost for capacity scenario 2. From an economic  
549 perspective, this comparison shows that deployment of OCC systems is more cost-effective  
550 than the use of FAME. Therefore, OCC systems designed based on small capacity scenarios 1–  
551 2 are identified as the optimal capacities of the OCC system in terms of the CO<sub>2</sub> avoidance cost  
552 and the CO<sub>2</sub> avoided rate.

553 In order to generalize the optimal capacity of the OCC system identified using the actual main  
554 engine load profile, this study generated hypothetical main engine load profiles with a  
555 consistent average load of 49% but different distributions (Appendix B. Hypothetical profiles).  
556 Table 9 shows the cumulative performance calculated for their different profiles. Consistent  
557 with the findings from the actual profile, OCC systems based on capacity scenarios 1–2 are  
558 also observed as optimal capacities in most of the other generated profiles. However, while the  
559 overall trend is consistent, there can be a large deviation in derived cumulative performance  
560 depending on the distribution of load profiles. This is because the load profile determines two  
561 main factors. The frequency of each engine load and whether each capture system would

562 operate within its available operating range. These factors directly affect the cumulative  
 563 performance by either increasing or decreasing the carbon reduction potential of capture  
 564 systems. Thus, the design approach for OCC systems should reflect flexible ship operation  
 565 (actual engine load profile) to avoid oversized equipment and unnecessary capital investment,  
 566 and to accurately calculate cumulative performance.

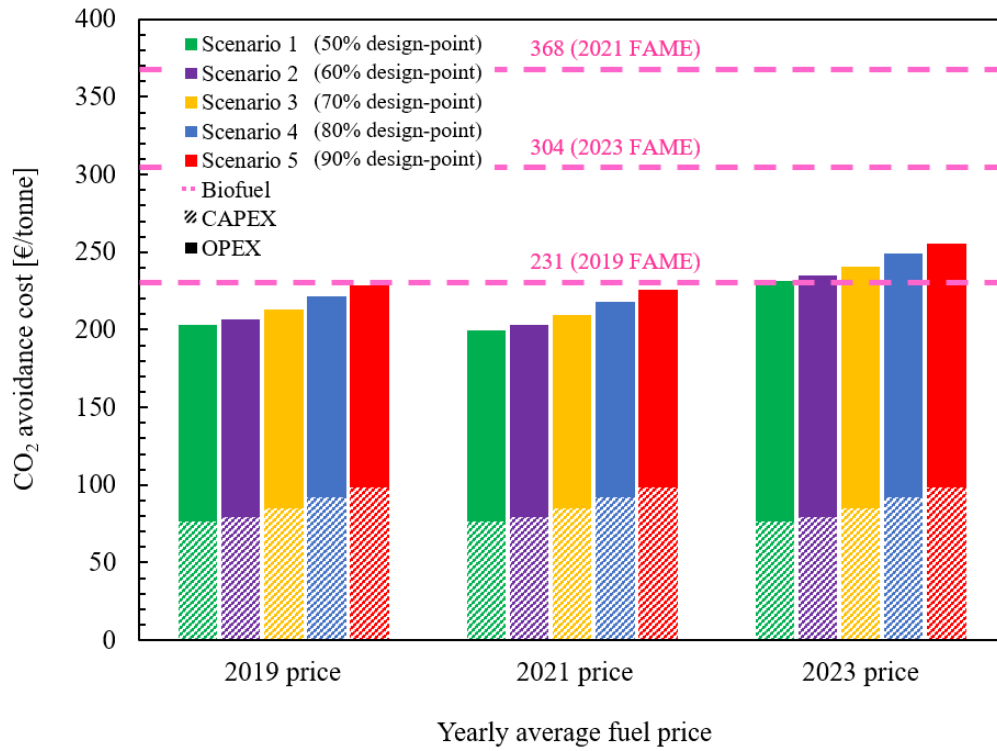
567

568 Table 8. Cumulative performance of the target ship with the onboard carbon capture systems  
 569 over a single voyage.

Category	Unit	Target ship w/o OCC	Capacity scenario 1	Capacity scenario 2	Capacity scenario 3	Capacity scenario 4	Capacity scenario 5
Design-point load	%	-	50	60	70	80	90
CO <sub>2</sub> generated (total)	tonne/hr	3.56	4.44	4.48	4.46	4.40	4.39
CO <sub>2</sub> generated (main engine)	tonne/hr	3.56	3.56	3.56	3.56	3.56	3.56
CO <sub>2</sub> generated (additional)	tonne/hr	-	0.87	0.92	0.89	0.84	0.83
CO <sub>2</sub> captured	tonne/hr	-	2.86	3.01	2.96	2.82	2.83
CO <sub>2</sub> emitted	tonne/hr	3.56	1.57	1.47	1.49	1.58	1.56
CO <sub>2</sub> avoided	tonne/hr	-	1.99	2.09	2.07	1.99	2.00
CO <sub>2</sub> avoided rate	%	-	56	59	58	56	56
Cumulative SEC of CO <sub>2</sub> avoided	GJ <sub>th</sub> /tonne	-	3.14	3.14	3.08	3.01	2.91
CO <sub>2</sub> avoidance cost	€/tonne	-	232	235	241	249	256
CAPEX	€/tonne	-	77	79	85	92	98
FOPEX	€/tonne	-	47	47	50	53	55
VOPEX* <sup>1</sup>	€/tonne	-	108	108	106	104	102

570 \*<sup>1</sup> based on 2023 MGO price

571



572

573

Fig. 13. CO<sub>2</sub> avoidance cost of the onboard carbon capture system compared to the alternative decarbonization strategy.

574

575



Table 9. Cumulative performance for different ship profiles.

Category	Hypothetical profile 1		Hypothetical profile 2 (similar to actual profile)		Hypothetical profile 3 (similar to actual profile)	
	CO <sub>2</sub> avoidance cost	CO <sub>2</sub> avoided rate	CO <sub>2</sub> avoidance cost	CO <sub>2</sub> avoided rate	CO <sub>2</sub> avoidance cost	CO <sub>2</sub> avoided rate
	(€/tonne)	(%)	(€/tonne)	(%)	(€/tonne)	(%)
Scenario 1	247	42	232	57	237	55
Scenario 2	264	44	235	59	243	58
Scenario 3	289	43	237	60	243	58
Scenario 4	288	46	248	56	250	56
Scenario 5	290	49	255	56	257	56

## 578        **7. Conclusions**

579        This study investigated the performance of the MEA-based OCC system under varying  
580 exhaust gas conditions of marine engines, reflecting an actual sailing profile. Based on the  
581 cumulative performance, this work focused on identifying the optimal capacity of the capture  
582 systems to avoid oversized equipment and unnecessary capital investment, which can be an  
583 obstacle to quick deployment of carbon capture systems in the marine industry. The target  
584 vessel was an LNG-fueled container ship powered by a two-stroke low-pressure dual-fuel  
585 engine, considering the high CO<sub>2</sub> emissions from the marine segment and the growing market  
586 share of the engine type. In particular, the results of the case study indicate that OCC systems  
587 are more cost-effective than the use of FAME, even under the worst assumptions considering  
588 the characteristics of NG-fired two-stroke engine (low exhaust gas temperature and CO<sub>2</sub>  
589 concentration compared to four-stroke engines).

590        The smaller OCC systems can achieve a similar level of CO<sub>2</sub> reduction to other larger capture  
591 systems when the average engine load is low. For this load profile, smaller capture systems  
592 should vent some of the exhaust gas at high engine loads. However, by setting a lower design-  
593 point load, the operating range of the absorber can be extended to the low engine load region,  
594 where the frequency is much higher than the high load region. Thus, they can handle a wider  
595 load range than larger capture systems, which offsets the CO<sub>2</sub> loss. This makes it possible to  
596 reduce the CO<sub>2</sub> avoidance cost by decreasing CAPEX while maintaining the CO<sub>2</sub> avoided rate.  
597 Therefore, this study provides a new approach for designing appropriately sized amine-based  
598 OCC systems on a ship where space is limited.

599        It is, however, worth noting that the CO<sub>2</sub> avoided rate of the OCC system is limited to below  
600 60% regardless of the capacity, which will not be sufficient to achieve deep decarbonization of  
601 the shipping industry. The relatively low emission reduction potential is due to the narrow

602 operating range of the capture system under varying engine loads, which is constrained by the  
603 turndown ratio (2.5:1). In this study, a turndown ratio of 4:1 is required to cover the entire  
604 engine load variation when the OCC system is designed for 90% engine load. However,  
605 increasing the turndown ratio will be challenging under shipboard conditions due to equipment  
606 height limitations and motion dynamics. Therefore, determining a feasible turndown ratio is  
607 expected to be essential to improve the capture potential and the economic viability of amine-  
608 based onboard carbon capture systems.

609 Another key aspect in designing and evaluating onboard capture systems is the engine load  
610 profile of a voyage. The load profile will vary depending on various factors such as vessel type,  
611 engine type, sailing route, and weather conditions. Thus, in this work, both design-point and  
612 off-design performance is quantified in advance so that any sailing profiles can be applied to  
613 evaluate the cumulative KPIs. This methodology is also expected to offer a suitable engine load  
614 profile when onboard carbon capture systems are implemented on a target vessel, increasing  
615 the emission reduction potential.

616 This work initially focused on the optimal capacity of an OCC system to minimize capital  
617 investment. However, both CAPEX and OPEX are found to be equally important to the CO<sub>2</sub>  
618 avoidance cost. In particular, the low temperature exhaust gas from two-stroke engines results  
619 in a relatively small amount of waste heat to be recovered, increasing fuel consumption for  
620 additional heat generation onboard. Therefore, further efforts are necessary to reduce the OPEX  
621 of capture systems, such as optimizing the onboard heat exchange network and increasing the  
622 exhaust gas temperature with minimal engine efficiency loss.

623

624 **Appendix A. Model validation**

625 The validation was performed by comparing the key simulation results, such as lean and rich  
 626 CO<sub>2</sub> loadings, CO<sub>2</sub> capture rate, and reboiler heat duty, with the pilot plant data (Table A. 1)  
 627 and then adjusting key factors (Table A. 2). The validated rate-based model yielded simulation  
 628 results that are similar to the experimental data, as shown in Table A. 1. The correlations and  
 629 tuning factors used for the validated rate-based model are summarized in Table A. 2.

630

631 **Table A. 1. Comparison of key simulation results with pilot plant data.**

Category	Unit	Pilot plant data [34]	Validated model	Absolute percentage error (%)
Flue gas	kg/h		72.1	-
CO <sub>2</sub>	mol%		3.5	-
H <sub>2</sub> O			7.6	-
N <sub>2</sub>			75.8	-
O <sub>2</sub>			13.1	-
Lean loading	mol CO <sub>2</sub> /mol MEA	0.232	0.232	0.1
Rich loading		0.310	0.313	1.3
CO <sub>2</sub> capture rate	%	84.6	84.9	0.3
Reboiler heat duty	kW	6.70	7.36	10.0

632

633 **Table A. 2. Specifications of the validated rate-based model.**

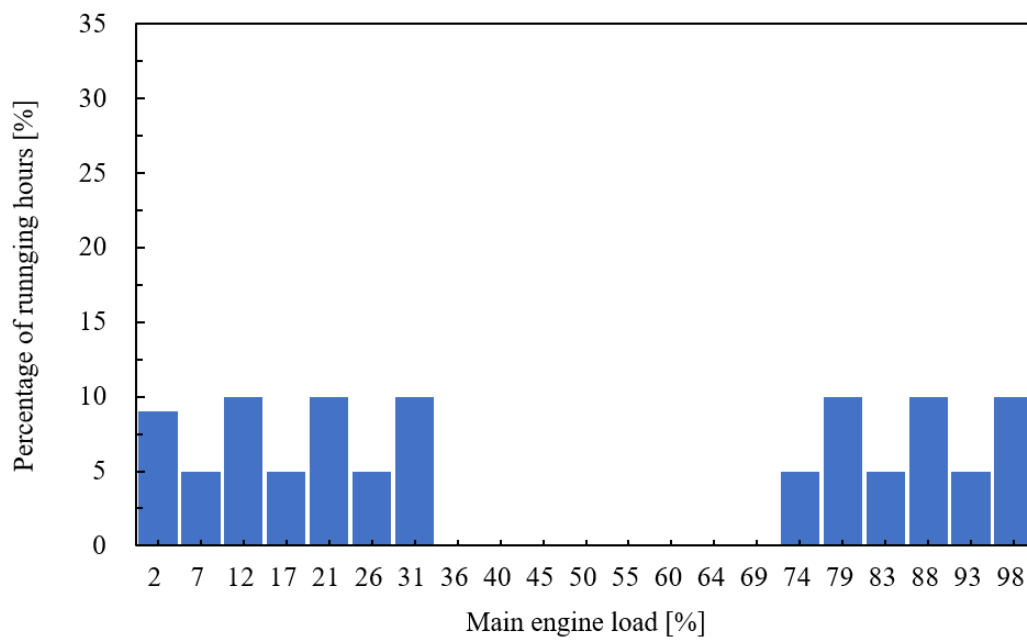
Category	Value
Calculation type	Rate-based calculation
Packing material	Mellapak 250Y [34,37]
Reaction condition factor	0.7
Film discretization ratio	5

Flow model	VPlug
Interfacial area factor	1.2
Mass transfer coefficient method	Brf-85 [54]
Heat transfer coefficient method	Chilton and Colburn [55]
Interfacial area method	Brf-85 [54]
Holdup method	Brf-92 [56]
Film resistance	Discrxn for liquid film; Film for vapor film

634

635 **Appendix B. Hypothetical profiles**

636

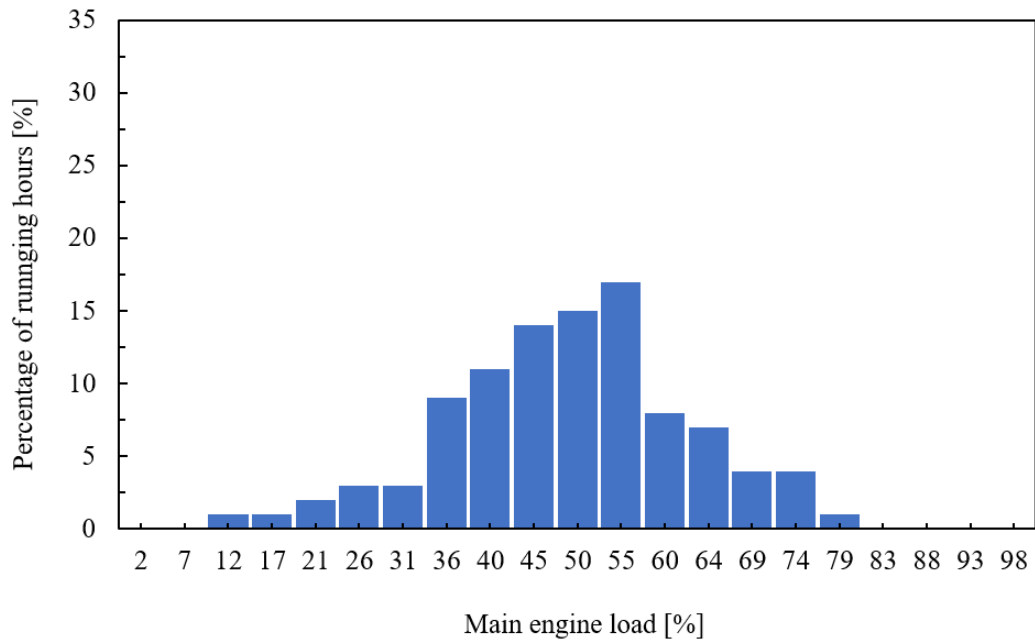


637

638

Fig. B. 1. Hypothetical profile 1.

639

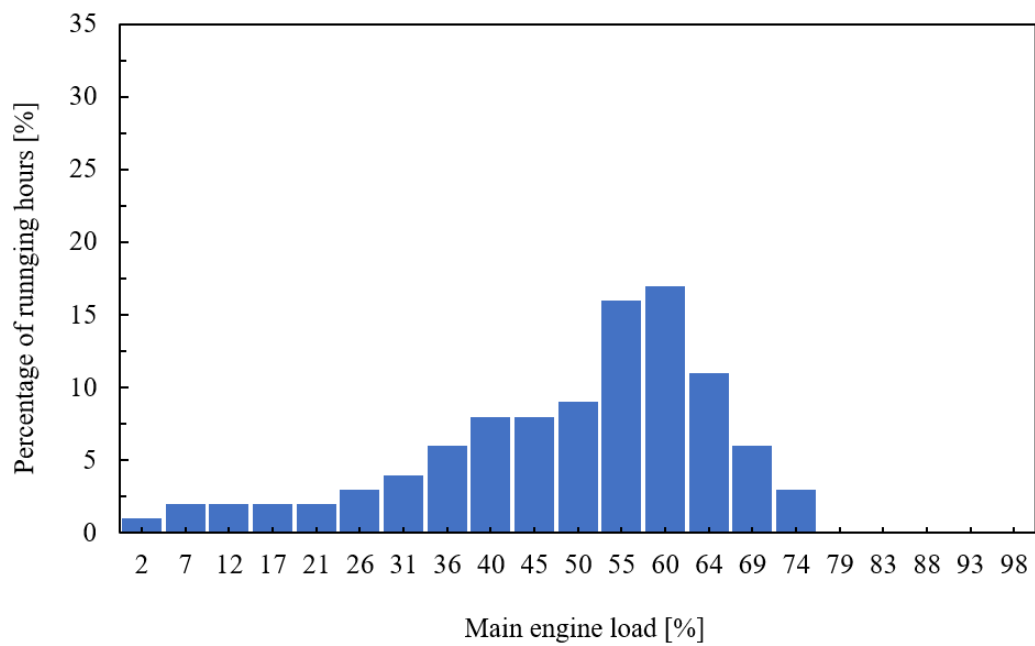


640

641

Fig. B. 2. Hypothetical profile 2.

642



643

644

Fig. B. 3. Hypothetical profile 3.

645

646 **CRedit authorship contribution statement**

647 **Juyoung Oh:** Conceptualization, Methodology, Analysis, Writing – Original Draft, Writing –  
648 Review & Editing, Visualization. **Donghoi Kim:** Conceptualization, Methodology, Analysis,  
649 Writing – Review & Editing. **Simon Roussanaly:** Conceptualization, Methodology, Analysis,  
650 Writing – Review & Editing. **Rahul Anantharaman:** Conceptualization, Methodology,  
651 Analysis, Writing – Review & Editing. **Youngsub Lim:** Conceptualization, Methodology,  
652 Analysis, Writing – Review & Editing, Supervision

653

654 **Declaration of Competing Interest**

655 The authors declare that they have no known competing financial interests or personal  
656 relationships that could have appeared to influence the work reported in this paper.

657

658 **Acknowledgments**

659 This work was supported by Korea Institute for Advancement of Technology (KIAT) grant  
660 funded by the Korea Government (MOTIE) (P0017304, Human Resource Development  
661 Program for Industrial Innovation) and the Korea Research Institute of Ships and Ocean  
662 engineering, grant from Endowment Project of “Technology Development of Onboard Carbon  
663 Capture and Storage System and Pilot Test” funded by Ministry of Oceans and Fisheries  
664 (PES4750). This work was also supported by the KSP project CCSShip under the MAROFF  
665 program of the Research Council of Norway (RCN project number 320260). The authors would  
666 like to acknowledge the following partners for their support: the NCCS Research Centre and  
667 its partners (Aker Carbon Capture, Allton, Ansaldo Energia, Baker Hughes, CoorsTek  
668 Membrane Sciences, Equinor, Fortum Oslo Varme, Gassco, KROHNE, Larvik Shipping,

669 Lundin Norway, Norcem, Norwegian Oil and Gas, Quad Geometrics, Stratum Reservoir, Total,  
670 Vår Energi, Wintershall DEA), Calix Limited, Klaveness, Wärtsilä, and the Research Council  
671 of Norway. The Research Institute of Marine Systems Engineering and Institute of Engineering  
672 Research at Seoul National University provided research facilities for this work.

673

## 674 **References**

- 675 [1] Scripps Institution of Oceanography, The Keeling Curve, 2022.  
676 <https://keelingcurve.ucsd.edu/> (accessed June 7, 2022).
- 677 [2] IMO, Fourth IMO GHG Study 2020, 2021.
- 678 [3] IMO, Amendments to the Annex of the Protocol of 1997 to Amend the International  
679 Convention for the Prevention of Pollution from Ships, 1973, as Modified by the  
680 Protocol of 1978 Relating Thereto (Inclusion of regulations on energy efficiency for  
681 ships in MARPOL Annex VI) (Resolution MEPC.203(62)), 2011.
- 682 [4] IMO, Report of the Marine Environment Protection Committee on its Seventy-Fourth  
683 Session, 2019.
- 684 [5] IMO, Resolution MEPC.304(72); Initial IMO strategy on reduction of GHG emissions  
685 from ships, 2018.
- 686 [6] IMO, 2021 Amendments to the Annex of the Protocol of 1997 to Amend the  
687 International Convention for the Prevention of Pollution from Ships, 1973, as Modified  
688 by the Protocol of 1978 Relating Thereto 2021 Revised MARPOL Annex VI (Resolution  
689 MEPC.328(76)), 2021.
- 690 [7] IMO, Report of the Marine Environment Protection Committee on its Seventy-Sixth  
691 Session, 2021.
- 692 [8] IMO, Resolution MEPC.377(80); 2023 IMO strategy on reduction of GHG emissions  
693 from ships, 2023.
- 694 [9] E.A. Bouman, E. Lindstad, A.I. Riialand, A.H. Strømman, State-of-the-art technologies,  
695 measures, and potential for reducing GHG emissions from shipping – A review, *Transp*  
696 *Res D Transp Environ.* 52 (2017) 408–421. <https://doi.org/10.1016/j.trd.2017.03.022>.
- 697 [10] J. Jung, Y. Seo, Onboard CO2 Capture Process Design using Rigorous Rate-based Model,  
698 *Journal of Ocean Engineering and Technology.* 36 (2022) 168–180.  
699 <https://doi.org/10.26748/ksoe.2022.006>.
- 700 [11] J.-Y. Park, J.-Y. Jung, Y.-T. Seo, Investigation of Applying Technical Measures for  
701 Improving Energy Efficiency Design Index (EEDI) for KCS and KVLCC2, *Journal of*



- 702 Ocean Engineering and Technology. 37 (2023) 58–67.  
703 <https://doi.org/10.26748/KSOE.2023.001>.
- 704 [12] IMO, Report of the Marine Environment Protection Committee on its Seventy-Eighth  
705 Session, 2022.
- 706 [13] J. Gardemal, American Bureau of Shipping MEPC 79 Brief, 2022.  
707 [https://safety4sea.com/wp-content/uploads/2022/12/ABS-MEPC-79-Brief-](https://safety4sea.com/wp-content/uploads/2022/12/ABS-MEPC-79-Brief-2022_12.pdf)  
708 [2022\\_12.pdf](https://safety4sea.com/wp-content/uploads/2022/12/ABS-MEPC-79-Brief-2022_12.pdf) (accessed February 16, 2023).
- 709 [14] M. Steyn, J. Oglesby, G. Turan, A. Zapantis, R. Gebremedhin, N. Al Amer, I. Havercroft,  
710 R. Ivory-Moore, X. Yang, M. Abu Zahra, E. Pinto, D. Rassool, E. Williams, C. Consoli,  
711 J. Minervini, Global Status of CCS 2022, 2022.  
712 [https://status22.globalccsinstitute.com/wp-content/uploads/2022/12/Global-Status-of-](https://status22.globalccsinstitute.com/wp-content/uploads/2022/12/Global-Status-of-CCS-2022_Download_1222.pdf)  
713 [CCS-2022\\_Download\\_1222.pdf](https://status22.globalccsinstitute.com/wp-content/uploads/2022/12/Global-Status-of-CCS-2022_Download_1222.pdf) (accessed February 16, 2023).
- 714 [15] American Bureau of Shipping, Setting the course to low carbon shipping: 2030 outlook  
715 2050 vision, 2019.
- 716 [16] J. Oh, R. Anantharaman, U. Zahid, P. Lee, Y. Lim, Process design of onboard membrane  
717 carbon capture and liquefaction systems for LNG-fueled ships, Sep Purif Technol. 282  
718 (2022) 120052. <https://doi.org/10.1016/j.seppur.2021.120052>.
- 719 [17] H.F. Svendsen, E.T. Hessen, T. Mejdell, Carbon dioxide capture by absorption,  
720 challenges and possibilities, Chemical Engineering Journal. 171 (2011) 718–724.  
721 <https://doi.org/10.1016/j.cej.2011.01.014>.
- 722 [18] M.G. Plaza, F. Rubiera, Development of carbon-based vacuum, temperature and  
723 concentration swing adsorption post-combustion CO<sub>2</sub> capture processes, Chemical  
724 Engineering Journal. 375 (2019). <https://doi.org/10.1016/j.cej.2019.122002>.
- 725 [19] B. Adhikari, C.J. Orme, C. Stetson, J.R. Klaehn, Techno-economic analysis of carbon  
726 dioxide capture from low concentration sources using membranes, Chemical  
727 Engineering Journal. 474 (2023). <https://doi.org/10.1016/j.cej.2023.145876>.
- 728 [20] Y. Kim, J. Lee, H. Cho, J. Kim, Novel cryogenic carbon dioxide capture and storage  
729 process using LNG cold energy in a natural gas combined cycle power plant, Chemical  
730 Engineering Journal. 456 (2023). <https://doi.org/10.1016/j.cej.2022.140980>.
- 731 [21] X. Luo, M. Wang, Study of solvent-based carbon capture for cargo ships through process  
732 modelling and simulation, Appl Energy. 195 (2017) 402–413.  
733 <https://doi.org/10.1016/j.apenergy.2017.03.027>.
- 734 [22] M. Feenstra, J. Monteiro, J.T. van den Akker, M.R.M. Abu-Zahra, E. Gilling, E.  
735 Goetheer, Ship-based carbon capture onboard of diesel or LNG-fuelled ships,  
736 International Journal of Greenhouse Gas Control. 85 (2019) 1–10.  
737 <https://doi.org/10.1016/j.ijggc.2019.03.008>.
- 738 [23] S. Lee, S. Yoo, H. Park, J. Ahn, D. Chang, Novel methodology for EEDI calculation  
739 considering onboard carbon capture and storage system, International Journal of  
740 Greenhouse Gas Control. 105 (2021) 103241.

- 741 <https://doi.org/10.1016/j.ijggc.2020.103241>.
- 742 [24] N.V.D. Long, D.Y. Lee, C. Kwag, Y.M. Lee, S.W. Lee, V. Hessel, M. Lee, Improvement  
743 of marine carbon capture onboard diesel fueled ships, *Chemical Engineering and*  
744 *Processing - Process Intensification*. 168 (2021).  
745 <https://doi.org/10.1016/j.cep.2021.108535>.
- 746 [25] C. Ji, S. Yuan, M. Huffman, M.M. El-Halwagi, Q. Wang, Post-combustion carbon  
747 capture for tank to propeller via process modeling and simulation, *Journal of CO2*  
748 *Utilization*. 51 (2021). <https://doi.org/10.1016/j.jcou.2021.101655>.
- 749 [26] A. Awoyomi, K. Patchigolla, E.J. Anthony, Process and Economic Evaluation of an  
750 Onboard Capture System for LNG-Fueled CO<sub>2</sub> Carriers, *Ind Eng Chem Res*. 59 (2020)  
751 6951–6960. <https://doi.org/10.1021/acs.iecr.9b04659>.
- 752 [27] J.A. Ros, E. Skylogianni, V. Doedée, J.T. van den Akker, A.W. Vredeveltdt, M.J.G.  
753 Linders, E.L.V. Goetheer, J. G M-S Monteiro, Advancements in ship-based carbon  
754 capture technology on board of LNG-fuelled ships, *International Journal of Greenhouse*  
755 *Gas Control*. 114 (2022). <https://doi.org/10.1016/j.ijggc.2021.103575>.
- 756 [28] UNCTAD, REVIEW OF MARITIME TRANSPORT 2022., 2023.
- 757 [29] M. Stec, A. Tatarczuk, T. Iluk, M. Szul, Reducing the energy efficiency design index for  
758 ships through a post-combustion carbon capture process, *International Journal of*  
759 *Greenhouse Gas Control*. 108 (2021). <https://doi.org/10.1016/j.ijggc.2021.103333>.
- 760 [30] A. Einbu, T. Pettersen, J. Morud, A. Tobiesen, C.K. Jayarathna, R. Skagestad, G.  
761 Nysæther, Energy assessments of onboard CO<sub>2</sub> capture from ship engines by MEA-  
762 based post combustion capture system with flue gas heat integration, *International*  
763 *Journal of Greenhouse Gas Control*. 113 (2022).  
764 <https://doi.org/10.1016/j.ijggc.2021.103526>.
- 765 [31] IMO, Third IMO GHG Study 2014, 2015.
- 766 [32] Wärtsilä, WSD80 3800 Container Feeder DATASHEET, 2016.  
767 [https://cdn.wartsila.com/docs/default-source/product-files/sd/merchant/feeder/wsd80-](https://cdn.wartsila.com/docs/default-source/product-files/sd/merchant/feeder/wsd80-3800-container-feeder-ship-design-o-data-sheet.pdf)  
768 [3800-container-feeder-ship-design-o-data-sheet.pdf](https://cdn.wartsila.com/docs/default-source/product-files/sd/merchant/feeder/wsd80-3800-container-feeder-ship-design-o-data-sheet.pdf) (accessed July 28, 2022).
- 769 [33] J. Husebye, A.L. Brunsvold, S. Roussanaly, X. Zhang, Techno economic evaluation of  
770 amine based CO<sub>2</sub> capture: impact of CO<sub>2</sub> concentration and steam supply, *Energy*  
771 *Procedia*. 23 (2012) 381–390. <https://doi.org/10.1016/j.egypro.2012.06.053>.
- 772 [34] R. Notz, H.P. Mangalapally, H. Hasse, Post combustion CO<sub>2</sub> capture by reactive  
773 absorption: Pilot plant description and results of systematic studies with MEA,  
774 *International Journal of Greenhouse Gas Control*. 6 (2012) 84–112.  
775 <https://doi.org/10.1016/j.ijggc.2011.11.004>.
- 776 [35] AspenTech, ENRTL-RK Rate-Based Model of the CO<sub>2</sub> Capture Process by MEA using  
777 Aspen Plus - Version 10.0, Bedford, MA, USA, 2008. <http://www.aspentech.com>.
- 778 [36] H.Z. Kister, J.R. Haas, D.R. Hart, D.R. Gill, *Distillation Design*, McGraw-Hill, New  
779 York, 1992.

- 780 [37] E.O. Agbonghae, K.J. Hughes, D.B. Ingham, L. Ma, M. Pourkashanian, Optimal Process  
781 Design of Commercial-Scale Amine-Based CO<sub>2</sub> Capture Plants, (2014).  
782 <https://doi.org/10.1021/ie5023767>.
- 783 [38] M. Biermann, F. Normann, F. Johnsson, R. Skagestad, Partial Carbon Capture by  
784 Absorption Cycle for Reduced Specific Capture Cost, *Ind Eng Chem Res.* 57 (2018)  
785 15411–15422. <https://doi.org/10.1021/acs.iecr.8b02074>.
- 786 [39] Koch-Glitsch, PACKED TOWER Internals, 2020. [https://koch-glitsch.com/technical-](https://koch-glitsch.com/technical-documents/brochures/packed-tower-internals)  
787 [documents/brochures/packed-tower-internals](https://koch-glitsch.com/technical-documents/brochures/packed-tower-internals) (accessed April 8, 2023).
- 788 [40] H.Z. Kister, *Distillation Operation*, McGraw-Hill, 1990.
- 789 [41] Sulzer Chemtech, *Internals for packed columns*, 2010.
- 790 [42] WinGD, Marine Installation Manual X72DF, 2021.  
791 <https://www.wingd.com/en/search/?q=marine%20installation%20manual> (accessed  
792 June 27, 2023).
- 793 [43] S. Roussanaly, E.S. Rubin, M. Van der Spek, G. Booras, N. Berghout, T. Fout, M. Garcia,  
794 S. Gardarsdottir, V. Nair Kuncheekanna, M. Matuszewski, S. Mccoy, J. Morgan, S.  
795 Mohd Nazir, A. Ramirez, Towards improved guidelines for cost evaluation of carbon  
796 capture and storage-a white paper, 2021.
- 797 [44] S.G. Subraveti, S. Roussanaly, R. Anantharaman, L. Riboldi, A. Rajendran, How much  
798 can novel solid sorbents reduce the cost of post-combustion CO<sub>2</sub> capture? A techno-  
799 economic investigation on the cost limits of pressure–vacuum swing adsorption, *Appl*  
800 *Energy.* 306 (2022). <https://doi.org/10.1016/j.apenergy.2021.117955>.
- 801 [45] S. Roussanaly, N. Berghout, T. Fout, M. Garcia, S. Gardarsdottir, S.M. Nazir, A. Ramirez,  
802 E.S. Rubin, Towards improved cost evaluation of Carbon Capture and Storage from  
803 industry, *International Journal of Greenhouse Gas Control.* 106 (2021).  
804 <https://doi.org/10.1016/j.ijggc.2021.103263>.
- 805 [46] Bunker Index, Bunker Index: Rotterdam, Netherlands, 2023.  
806 <https://bunkerindex.com/index.php> (accessed June 13, 2023).
- 807 [47] S.O. Gardarsdottir, E. De Lena, M. Romano, S. Roussanaly, M. Voldsund, J.F. Pérez-  
808 Calvo, D. Berstad, C. Fu, R. Anantharaman, D. Sutter, M. Gazzani, M. Mazzotti, G.  
809 Cinti, Comparison of Technologies for CO<sub>2</sub> Capture from Cement Production—Part 2:  
810 Cost Analysis, *Energies (Basel).* 12 (2019). <https://doi.org/10.3390/en12030542>.
- 811 [48] Neste, Biodiesel prices (SME & FAME), 2023.  
812 <https://www.neste.com/investors/market-data/biodiesel-prices-sme-fame#f29d80dc>  
813 (accessed June 13, 2023).
- 814 [49] S. Roussanaly, Calculating CO<sub>2</sub> avoidance costs of Carbon Capture and Storage from  
815 industry, *Carbon Manag.* 10 (2019) 105–112.  
816 <https://doi.org/10.1080/17583004.2018.1553435>.
- 817 [50] R. Notz, I. Tönnies, H.P. Mangalapally, S. Hoch, H. Hasse, A short-cut method for  
818 assessing absorbents for post-combustion carbon dioxide capture, *International Journal*

- 819 of Greenhouse Gas Control. 5 (2011) 413–421.  
820 <https://doi.org/10.1016/j.ijggc.2010.03.008>.
- 821 [51] S. Freguia, G.T. Rochelle, Modeling of CO<sub>2</sub> Capture by Aqueous Monoethanolamine,  
822 *AIChE Journal*. 49 (2003) 1676–1686. <https://doi.org/10.1002/aic.690490708>.
- 823 [52] OGCI and Stena Bulk, Is carbon capture on ships feasible?, 2021.  
824 [https://www.ogci.com/wp-](https://www.ogci.com/wp-content/uploads/2021/11/OGCI_STENA_MCC_November_2021.pdf)  
825 [content/uploads/2021/11/OGCI\\_STENA\\_MCC\\_November\\_2021.pdf](https://www.ogci.com/wp-content/uploads/2021/11/OGCI_STENA_MCC_November_2021.pdf) (accessed  
826 February 16, 2023).
- 827 [53] DNV, Use of biofuels in shipping, 2023. [https://www.dnv.com/news/use-of-biofuels-in-](https://www.dnv.com/news/use-of-biofuels-in-shipping-240298)  
828 [shipping-240298](https://www.dnv.com/news/use-of-biofuels-in-shipping-240298) (accessed June 30, 2023).
- 829 [54] J.L. Bravo, J.A. Rocha, J.R. Fair, Mass transfer in gauze packings, *Hydrocarbon*  
830 *Processing*. 64 (1985) 91–95.
- 831 [55] R. Taylor, R. Krishna, Multicomponent mass transfer, John Wiley & Sons, New York,  
832 1993.
- 833 [56] J.L. Bravo, J.A. Rocha, J.R. Fair, A comprehensive model for the performance of  
834 columns containing structured packings, *Institution of Chemical Engineers Symposium*  
835 *Series*. 129 (1992) A439.
- 836